Scanning Microscopy

Volume 1995
Number 9 *Luminescence*

Article 2

1995

Thermoluminescence of Zircon

Philibert Iacconi
Université de Nice-Sophia Antipolis, iacconi@unice.fr

Scanning Microscopy Supplement 9, 1995 (Pages 13-34) 0892-953X/95$5.00+.25
Scanning Microscopy International, Chicago (AMF O'Hare), IL 60666 USA

THERMOLUMINESCENCE OF ZIRCON

Philibert Iacconi

Lab. de Physique Electronique des Solides, Centre de Rech. sur les Solides et leurs Applications, LPES-CRESA, Faculté des Sciences, Université de Nice-Sophia Antipolis, 06108 Nice Cedex 2, France

Telephone number: (33) 4 9207 6331 / FAX number: (33) 4 9207 6336 / E.Mail: iacconi@unice.fr

Abstract

The thermoluminescence (TL) of synthetic zircons into which some impurities have been individually inserted is investigated. The results obtained show that, after X-irradiation at 77K, the synthetic zircons present three kinds of thermoluminescent emissions. The first is related to the OH^- ions, the second is typical of the SiO_4^{4-} groups, and the third is characteristic of RE^{3+} ions with RE = Dy, Tb, Gd, Eu, or Sm (RE = rare earth).

The OH^- emission is a large band at 285 nm which appears at 115 and 160K.

The SiO_4^{4-} TL emission consists of a 365 nm band observed at 100, 165, 205, 260, and 325K. The mechanisms associated with these TL peaks are fairly well described in terms of an electron trapped in the field of two positive charges, one substituted to silicon ion, the other to a neighbouring oxygen ion.

For temperatures up to 350K, the characteristic emissions of RE^{3+} are the consequence of an energy transfer mechanism from the TL emission as a result of recombination in SiO_4^{4-} host groups or OH^- centres to the RE^{3+} emitting activators. At temperatures higher than 350K, there are also some other RE^{3+} characteristic peaks which are interpreted in terms of charge transfer mechanisms.

The systematic compilation of results obtained with a series of natural zircons from various origins shows that the main TL properties are explained by the mechanisms described above.

Key Words: Synthetic and natural zircons, thermoluminescence, trapping and emission centres, defects and impurities in crystal, radiation damages, irradiation effects, metamictisation.

Introduction

When they are heated, some natural minerals such as zircon, quartz, etc., exhibit the so-called thermoluminescence (TL) phenomenon [56]. Usually, they are large gap materials and contain several kinds of lattice defects (imperfections, impurities) which are able to trap charge carriers.

The TL process requires two stages. In the first step, free electrons and holes are produced by ionising radiations and diffuse through the crystal until they are attracted by lattice defects, in which they remain hold as long as the temperature is not raised. For example, an electron can be trapped in a negative ion vacancy and a hole in the site of a cation vacancy. In terms of energy band scheme, these defects are related to energy levels allowed in the so-called forbidden band (Fig. 1). The second step consists to heat the mineral in order to provide it with enough energy to evict the trapped charges from their traps. The released charges can fall back to their stable position. For instance, the ejected electron can diffuse through the conduction band and recombine with a trapped hole. If the recombination is radiative, the energy of recombination is given out in the form of light called thermoluminescence. The TL model described here is the simplest model of TL. Other series of processes can also take place [57]. As regards the manner by which the irradiation is given out, one can discern: the natural TL in which the irradiation is provided by natural radiations {cosmic rays, ultra-violet (UV) solar light, radioactive elements, etc.} and the artificial TL in which the formation of TL centres is caused thanks to laboratory ionising radiation sources.

As long as the irradiation does not destroy the lattice structure, the intensity of TL increases with a prolonged exposure to the radiations. This property is used in archaeometry [2, 3, 80], geology dating [90] and in ionising radiation dosimetry by TL [64].

In a given lattice, each TL peak is characteristic of one lattice defect. So, TL can be also used for the characterisation of materials [46].

Several studies have shown that the natural zircon is

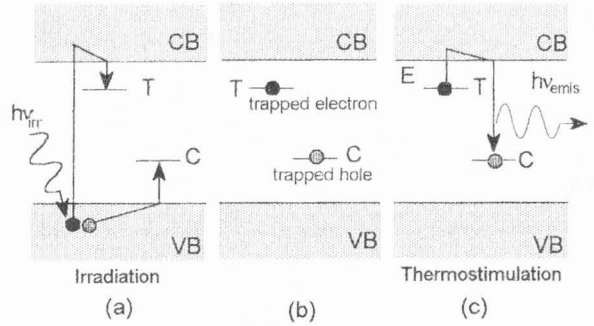

Figure 1. Diagram of energy levels describing the mechanisms of TL phenomenon in the case of crystal containing only two kinds of defects giving rise to one electron trap T and one recombination centre C.

(a) Electron and hole trapping. Ionising radiation of $h\nu_{irr}$ energy is absorbed in the material; free holes and electrons are produced and trapped at defects C and T, respectively.

(b) As long as they do not acquire sufficient energy to escape, the trapped holes and electrons remain in their traps. The lifetime τ of the electrons in the traps is determined by the trap depth E and the crystal temperature.

(c) Thermostimulation. When the temperature of material is raised, trapped electrons may acquire sufficient energy to escape. The released electrons may recombine with the holes at luminescent centre C and, if the recombination is radiative, light is emitted with energy $h\nu_{emis}$ and TL curve can be observed.

---

thermoluminescent [16, 38, 44, 45, 48, 49, 75]. The obtained TL curves are difficult to interpret because the role of trapping or luminescence centres can be played by the numerous impurities included in the natural zircon lattice. Besides, natural zircons also contain traces of radioactive elements which maintain continual α-bombardment and cause structural damages (metamictisation).

It is generally admitted that the α-decay damage results in characteristic changes of physical properties, e.g., volume expansion, decrease in density, birefringence, optical transmission [35], and reduction of TL intensity [91]. Usually, zircons are classified as high density (4.7) or low density (3.9) zircons. The high density zircon is transparent or semitransparent, weakly coloured, and has refractive indices of 1.92 and 1.98 with a birefringence of 0.06. It is regarded almost completely as crystalline zircon, containing a small amount of radiation damage [103]. In contrast, low density zircon has darker colour or is almost opaque. It has lower refractive indices (1.78 and 1.82) and its birefringence is smaller ($\approx$ 0.005). Low density zircon corresponds to

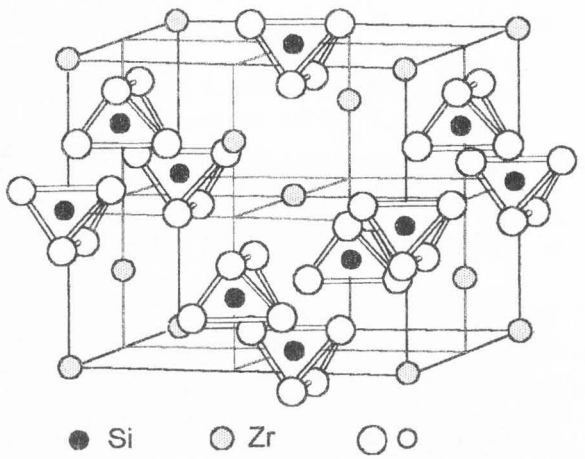

Figure 2. The tetragonal unit cell of $ZrSiO_4$. After Wyckoff [102].

---

highly metamict state [103]. There are also intermediate types with intermediate physical properties (the semi-metamict zircons)

In order to study the role played by each kind of defects, it is better to investigate the TL of synthetic zircons where each kind of impurity is individually inserted.

The aims of this work are: (1) to summarize the main results obtained from the investigation of doped or undoped synthetic zircon TL; (2) to describe the main TL properties of natural zircons and to interpret them by comparison with synthetic zircon TL results; and (3) to investigate the radiation damage in natural zircons in relation with the TL phenomena.

Crystallography

Zircon (orthosilicate of zirconium, $ZrSiO_4$) crystallises in the D_{4h}^{19} space group [102]. Its tetragonal unit cell, with a_o = 0.6607 nm and c_o = 0.5982 nm [72], contains four molecules (Fig. 2), and its structure consists of interlocking SiO_4 and ZrO_4 tetrahedra (Fig. 3). Each Si^{4+} ion is located at the centre of a deformed tetrahedron of O^{2-} ions and each Zr^{4+} is at the centre of two tetrahedra of O^{2-} ions (Fig. 3) such that four of the oxygen atoms are at 0.2131 nm and four at 0.2268 nm [72]. Oxygen is coordinated by one Si at 0.1622 nm. Each SiO_4 tetrahedron is isolated, the linkage being made through the zirconium atom to another SiO_4 tetrahedron [97]. Si and Zr sites have the same point symmetry D_{2d}.

Natural zircons usually contain trivalent rare-earth ions (RE^{3+}), uranium, thorium and radiogenic elements and also other substituents necessary for charge balance [79].

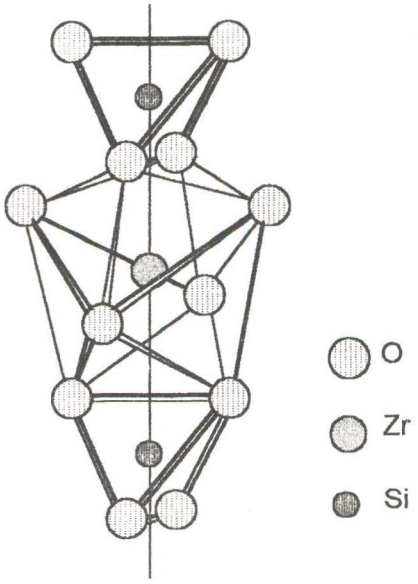

Figure 3. The chain of alternating edge-sharing SiO_4 tetrahedra and ZrO_8 triangular dodecahedra in zircon. After Robinson *et al.* [72].

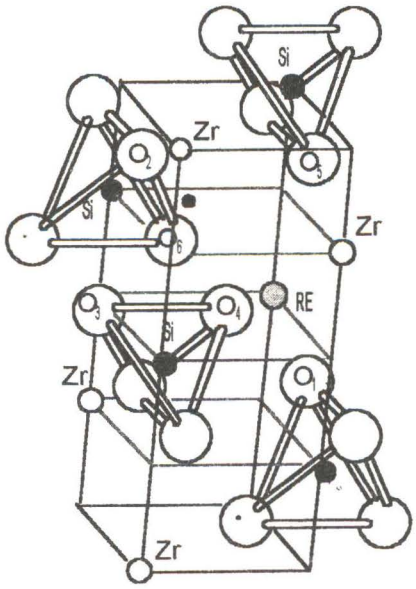

Figure 4. A part of the unit cell of zircon showing the positions of the ions of Zr, RE, H, and O. The oxygen O_1 is defective and the proton is linked to O_2. After Vinokurov *et al.* [92].

On the basis of comparative ionic radii, it is generally believed that the usual doping elements are located at the Zr^{4+} sites. This assumption is confirmed by numerous works using electron paramagnetic resonance (EPR) [7, 71, 73, 76, 77, 92] or luminescence [28] techniques. In natural zircons, the charge compensating mechanism is unknown as natural material contains many trace impurities. In the case of RE^{3+} doped synthetic zircon, the problem of maintaining electrical neutrality could mean that compensating ions in the proximity of the RE^{3+} ion produce localised distortions that change the site symmetry [28]. Three types of symmetry sites are identified in RE^{3+}-doped synthetic zircon. One of these, with the D_{2d} tetragonal symmetry, is assigned to ions substituted at Zr sites with the necessary charge compensation mechanism not disturbing the site symmetry [71]. Others have the orthorhombic symmetry (site symmetry not higher than C_2) and are of two types; the change in site symmetry is due to nearby charge compensation [71]. These results are confirmed by Votyakov *et al.* [94].

Various mechanisms of compensation charge have been proposed. At high concentrations of RE, when there is a high probability of substituting two RE in adjacent sites Zr, charge balance can be achieved by formation of O^- centres [7] with production of SiO_2^-, SiO_3^{3-}, SiO_4^{5-} radicals [78]. Vinokurov *et al.* [92] propose a model in which charge compensation is provided in $Zr^{4+} \rightarrow Y^{3+}$ substitution by OH^- replacing O^{2-} in the second coordination sphere (Fig. 4). Following Dawson *et al.* [19], the hydroxyl ions are in several different sites in the lattice. Caruba *et al.* [13] suggest charge balance by an $(OH)_4 \rightleftarrows SiO_4$ substitution which results in: $(Zr_{1-y}RE_y)(SiO_4)_{1-x}(OH)_{4x-y}$.

Experimental

Synthetic zircon samples studied have been synthesised and doped by a hydrothermal method in conditions close to the one of the natural zircon crystallisation.

Our investigations are focused on two synthetic zircon kinds called Z_O and Z_F, respectively. The first crystallises in $ZrSiO_4$ structure, but the presence of an infrared (IR) absorption at 3520 cm^{-1} lead us to attribute the formula $Zr(SiO_4)_{1-x}(OH)_{4x}$ to the hydroxylated zircon Z_F in which one SiO_4 group is replaced by one $(OH)_4$ tetrahedron [13]. The IR absorption band disappears when Z_F is annealed at 1100°C for 24 hours. In this case, Z_F is de-hydroxylated producing zircon Z_O, ZrO_2 and H_2O.

Zircon synthesis and doping methods have already been described [41, 43]. Investigations performed by the mean of classical methods such as EPR, IR absorption, etc., and, above all, thermoluminescence have allowed us to identify some luminescence and trapping centres involved in the synthetic zircon TL.

The TL measurements have been made between liquid nitrogen temperature (LNT) and 700K at a constant rate of 30K/min in a secondary vacuum or from room

temperature (RT) to 800K at the same heating rate in an air environment. The irradiation is performed *in situ*, at LNT or at RT, with an X-ray tube (W-target, 45 kV). The spectral analysis of TL peaks can be performed between 250 and 800 nm using 10 to 20 nm bandwidth interference filters. The experimental details are given in previous papers [41, 43].

Trapping and Emission Centres in X-Irradiated Synthetic Zircon

Contribution of OH^- ion [41]

Figure 5 shows the TL curves recorded after X-ray irradiation at 77K from unannealed and annealed undoped Z_F. It is observed that an unannealed undoped Z_F sample exhibits two intense TL peaks at 115K and 160K and a much weaker one at 340K. The comparison of the TL curves for unannealed and annealed Z_F reveals that, as a general rule, the effect of annealing is to reduce the intensity of the low temperature peaks ($T < 250K$) and to give rise to a peak at 325K or increase the one at 340K while shifting its maximum.

The decreasing of the TL intensity is very important for the 115K peak which has nearly disappeared. The decreasing of the low temperature peaks coincides with the de-hydroxylation of the sample. In other words, the presence of OH^- groups is responsible for the emission around 285 nm observed in the 115K and 160K TL peaks of unannealed hydroxylated zircons (Fig. 6). This emission band is broad, very unsymmetrical and shows several shoulders. The asymmetrical shape of the emission band and the presence of secondary maxima suggest that it has a vibronic character. The energy difference (0.43 eV) just corresponds to the O-H stretching energy in zircon [41]. After annealing, we observe the vanishing of the most energetically part of this spectral emission (Fig. 6). The 325K TL peak of annealed Z_F exhibits a 365 nm emission band (Fig. 7).

As it is shown by IR absorption, TL and EPR experiments [41], X-irradiation at 77K can lead to OH^- dissociation in two different ways:

$$OH^- + h\nu_X \rightarrow O^- + H^o \quad (1a)$$

$$OH^- + h\nu_X \rightarrow OH + e^- \quad (1b)$$

where neutral hydrogen H^o and electron e^- are removed from their initial sites, diffuse through the crystal lattice and are "frozen in" structure lattice defects of zircon where they remain trapped. Heating leads to the release of H^o at 115K:

$$H^o + O^- \rightarrow (OH^-)^* \rightarrow OH^- + h\nu_{em}\ (285\ nm) \quad (2a)$$

and, then, of trapped electron e^- at 160K according to:

$$OH + e^- \rightarrow (OH^-)^* \rightarrow OH^- + h\nu_{em}\ (285\ nm) \quad (2b)$$

In both cases, recombination is radiative and the existence of a common step for deexcitation explains the observed similarity in the emission spectra of both TL peaks.

The EPR measurements demonstrate clearly the presence of H^o in X-irradiated zircon and it disappearance for temperatures higher than 130K.

A non-assigned emission at 280 nm is observed by Votyakov *et al.* [93, 94] in X-ray excited luminescence of hydrothermal zircons. This band, relatively intense at 105K and predominant for temperature lower than 150K, vanishes progressively when the temperature of measurement is raised and disappears at about 350K. It probably originates from mechanisms described above.

Contribution of the SiO_4^{4-} groups [42]

The TL of nominally undoped $ZrSiO_4$ (Z_O) is mainly characterised by an emission band centred at 365 nm [42], observed in the 100K, 165K, 205K, 260K, and 350K TL peaks (Fig. 8). This band is similar to the one observed in annealed Z_F (Fig. 7) and is associated with Dy^{3+} emission (see the next section) due to the traces of Dy^{3+} present in our synthetic zircons. Two weak peaks which are made up by a dissymetric emission band peaking at 285 nm are also shown around 120K and 160K. They reveal the presence of a small amount of OH^- in the zircon lattice. An unidentified red emission around 780 nm with maxima at 168K, 280K and 385K is also observed. It could be due to Fe^{3+} ion as observed by Gaft *et al.* [31] in photoluminescence.

The near UV emission is reported in numerous works [25, 26, 70, 93, 94]. Fedorovskikh *et al.* [25, 26] observe this band in radioluminescence of $ZrSiO_4:Eu^{3+}$ [25] and in cathodoluminescence of zircons doped with Dy or Eu [26]. These authors notice that the maximum of this emission lies in the 340-380 nm region for RT and is displaced toward longer wavelengths (450-450 nm) when the temperature is reduced at 77K [26]. According to them, the UV emission, which appears also in $K_2ZrSi_2O_7$, would be apparently due to excitation of Zr-O chains.

The emission band observed by Votyakov *et al.* [93] at 350-380 nm in X-ray luminescence of synthetic zircons disappears when the temperature of measurement reaches 600K.

The near UV emission has been observed by cathodoluminescence for a great number of silicates [54], all of which, possess tetrahedral SiO_4^{4-} groups and we think, same as Leverenz [54], that this emission is specific to this group or, more generally, of the Si-O bond. It is an host lattice emission. We have verified that such an emission appears also in TL spectra of $HfSiO_4$ and $ThSiO_4$ (Fig. 9) synthesised in the same conditions as zircon [42].

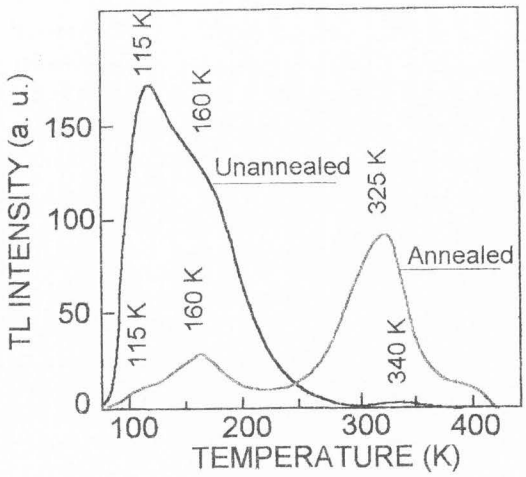

Figure 5. TL curves obtained from undoped Z_F zircon X-irradiated at LNT a) before and b) after annealing at 1375K for 24 hours [39].

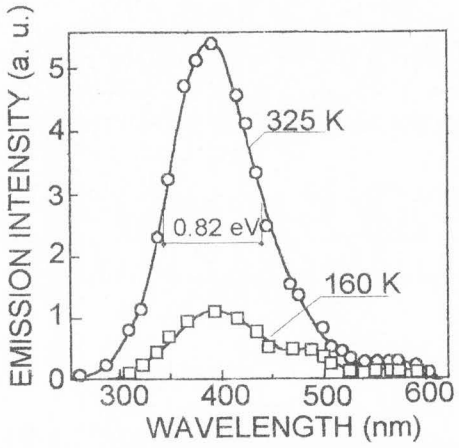

Figure 7. Emission spectra of the main TL peaks observed from undoped Z_F zircon after annealing at 1375K for 24 hours [40].

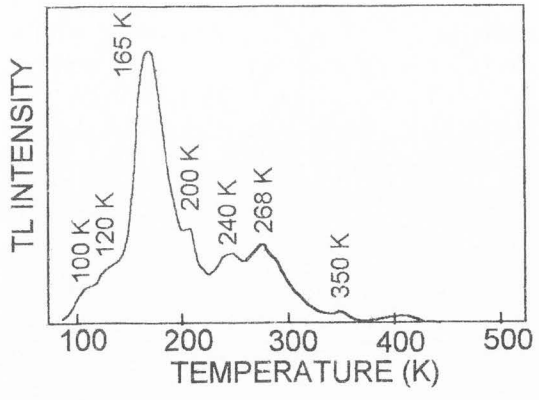

Figure 8. TL curve of undoped synthetic zircon Z_o after X-irradiation at LNT.

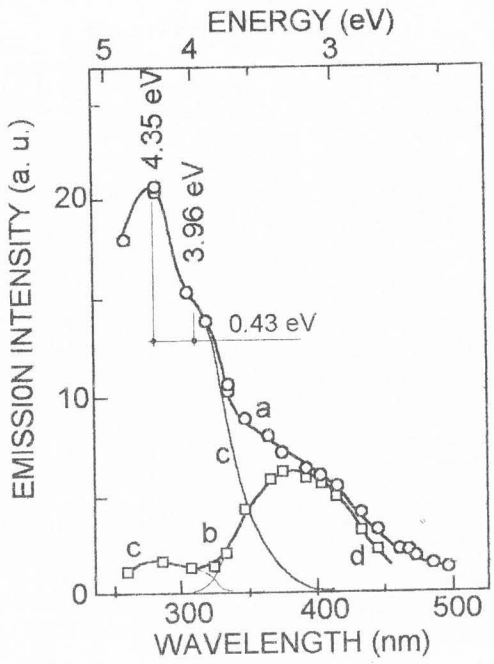

Figure 6. Spectral distribution for the 115K TL peak from an undoped Z_F sample a) before and b) after annealing (1375K, 24 hours), interpreted as resulting from an emission characteristic of the OH^- groups (curve c) and a 365 nm emission (curve d) [41].

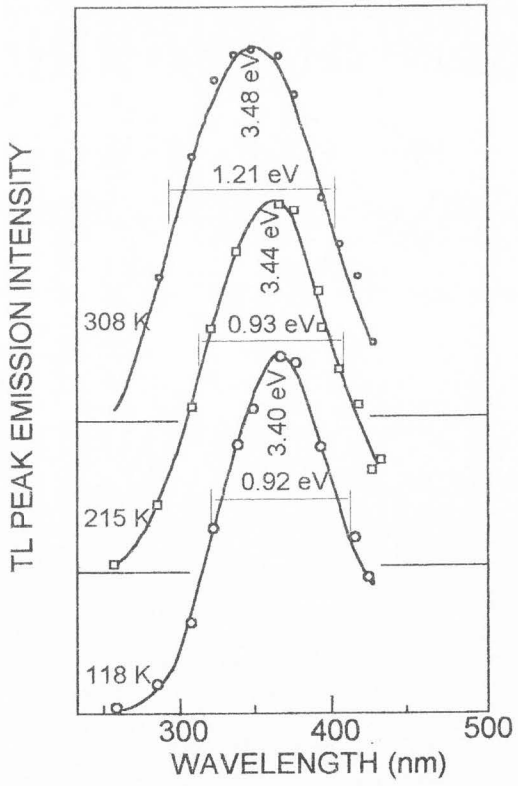

Figure 9. Host lattice emission observed from the TL peaks of undoped synthetic $ThSiO_4$ [40].

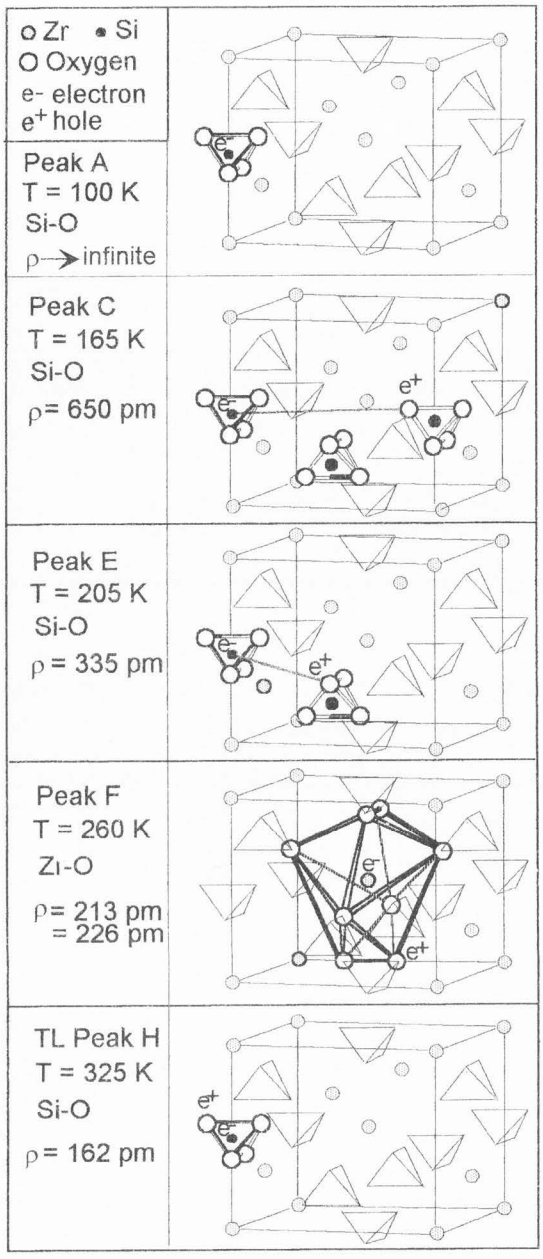

Figure 10. Diagram showing the proposed trapping centres.

Our interpretation is the following [42]: during the X-irradiation one outer shell electron is taken out from one SiO_4^{4-} group oxygen and transferred to one silicon ion where it remains trapped. In this case, the captured electron is placed in the field of two positive charges e^+, the one localised on oxygen ion which has lost the electron, the other on silicon ion. Various authors have noticed that, in SiO_4^{4-} tetrahedron, the effective valence of Si ion is close to +1 [10, 55, 67]. We can then use the H_2^+-like model proposed by Curie [18] resulting in:

Table 1. Comparison between predicted and observed E trap depth values of $ZrSiO_4$. The predicted values are calculated from eq. (5) and the observed values are determined from eq. (6). The uncertainties have been evaluated according to the standard deviation obtained for numerous measurements [40].

		E-values		TL peak	
	ρ	Predicted	Observed	Position	Peak
	nm	eV	eV	K	
Si-O	∞	0.23	0.15 ± 0.05	100	A
Si-O	0.650	0.39	0.36 ± 0.03	165	C
Si-O	0.335	0.54	0.49 ± 0.09	205	E
Zr-O	0.226	0.69	0.67 ± 0.07	260	F_2
Si-O	0.162	0.87	0.88 ± 0.08	325	H

$$E = \{(R/k_e^2) + (1/4\pi\epsilon_0 k)(e^2/\rho)\} \qquad (3)$$

where E corresponds to the trap depth and ρ to the distance between the two involved positive charges, R is the ionisation potential for the hydrogen atom, $\epsilon_0 k$ the static dielectric constant, and k_e an effective dielectric constant:

$$(1/k_e) = \{(1/k) + (5/16)\,[(1/k_0) - (1/k)]\} \qquad (4)$$

with $k_0 = n^2$, n being the index of refraction.

For zircon, k = 14, n ≈ 1.95, and eq. (3) becomes:

$$E(eV) = \{0.23 + [0.103/\rho(nm)]\} \qquad (5)$$

The existence of several trapping centres results from the several possible values of ρ (Fig. 10). The smallest E-value, 0.23 eV, is obtained for $\rho \to \infty$. The higher E-value, 0.87 eV, is obtained for the shortest value of ρ: 0.162 nm.

In as much as the peak at 260K is explained by a similar mechanism in which one of the two holes is localised on Zr^{4+} (in place of Si^{4+}) [42], this model is able to interpret the various TL peaks occurring in synthetic zircons in the 77K-350K temperature range and emitting the 365 nm-emission.

The assumption made to explain the 260K TL peak is supported by Solntsev and Shcherbakova [77] who have shown, by EPR measurements, that γ-irradiation of natural zircon results in simultaneous formation of two centre types: electron centres involving capture of an electron by a Zr^{4+} cation and hole centres involving loss of an electron by one of the oxygen atoms.

The theoretical values of trap depths calculated from eq. (5) are in good agreement with the experimental values (Table 1). Besides, a relation between the trap

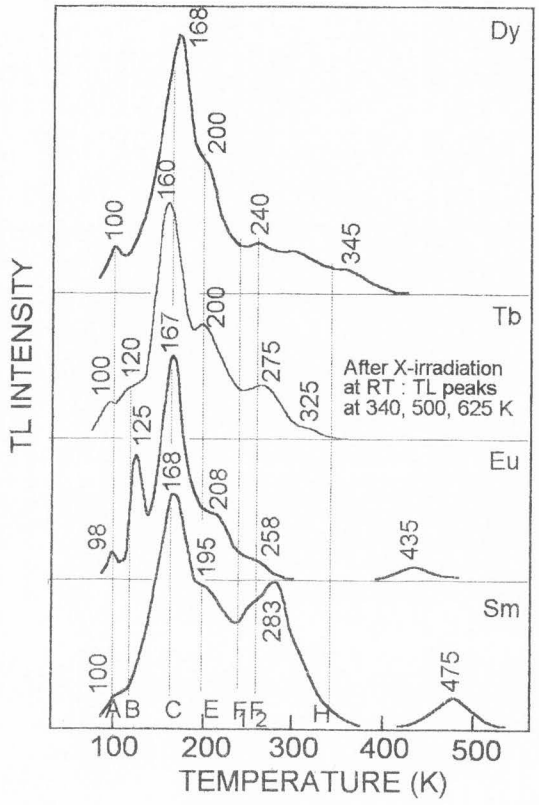

Figure 11. TL curves obtained after X-irradiation at LNT from some synthetic Z_o zircons respectively doped with Dy, Tb, Eu, and Sm.

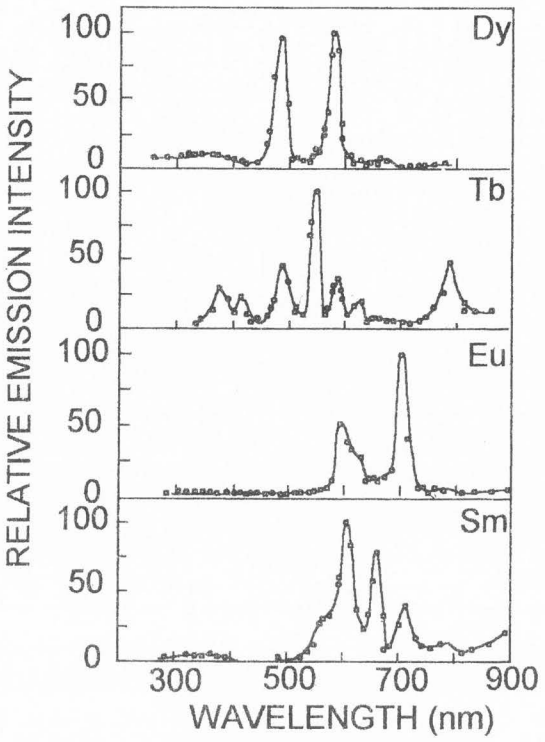

Figure 12. Emission spectra observed after X-irradiation at LNT from the main TL peak of some synthetic Z_o zircons respectively doped with Dy, Tb, Eu, and Sm.

---

depth E and the temperature T of TL peaks has been determined experimentally in the 77K-450K temperature range [40] and is approximately described by:

$$E(eV) = \{[T(K)-54] / 308\} \qquad (6)$$

The electron-hole recombination, occurring when the zircon sample is progressively heated, take place with an emission band situated near 365 nm. This mechanism involves only one luminescence centre type.

Influence of trivalent rare earth impurities [43]

77K-350K Temperature range The study of synthetic zircons (Z_F or Z_O) doped with individual rare earth elements of the lanthanide series such as Y^{3+}, La^{3+}, Ce^{3+}, Pr^{3+}, Nd^{3+}, Sm^{3+}, Eu^{3+}, Gd^{3+}, Tb^{3+}, Dy^{3+}, Ho^{3+}, Er^{3+}, Tm^{3+}, Yb^{3+}, Lu^{3+}, shows that only Dy^{3+}, Tb^{3+}, Gd^{3+}, Eu^{3+} and Sm^{3+} produce an important modification in the intensity of TL curves and are the cause of a characteristic RE^{3+} emission [43].

(a) Energy transfer from SiO_4^{4-} groups to Sm^{3+}, Eu^{3+}, Tb^{3+}, or Dy^{3+} ions After X-irradiation at 77K, zircons doped with Dy^{3+}, Tb^{3+}, Eu^{3+} or Sm^{3+} give rise to TL peaks at about 100K, 168K, 200K, and 345K (Fig. 11). All these peaks have emission spectra due to the concerned trivalent rare earth (RE^{3+}) activators (Fig. 12) which result from transitions within their incomplete 4f-shell. These emissions consist of groups of narrow lines unresolved by our measurement technique.

In $ZrSiO_4:Dy^{3+}$, the emission spectra of the TL peaks mentioned above are made up by three maxima peaking at 480, 580, and 662 nm, attributed to the $^4F_{9/2} \rightarrow {}^6H_{15/2}$, $^4F_{9/2} \rightarrow {}^6H_{13/2}$, and $^4F_{9/2} \rightarrow {}^6H_{11/2}$ transitions, respectively. The $^4F_{9/2} \rightarrow {}^6H_{9/2}$ transition, peaking at 760 nm, is also observed in some cases [40].

The spectral emission of TL peaks occurring in $ZrSiO_4:Tb^{3+}$ is similar to that of the main TL peak at 168K which consists in a set of emissions at 375, 416, 488, 545, 585, and 615 nm corresponding to the $^5D_3 \rightarrow {}^7F_{6,5}$ and $^5D4 \rightarrow {}^7F_{6,5,4,3}$ transitions, respectively, of Tb^{3+} ion.

The characteristic Eu^{3+} emission observed in $ZrSiO_4:Eu^{3+}$ is assigned to the transitions which take place from the $^5D_0$ excited level to the $^7F_1$ (595 nm), $^7F_2$ (615 nm), $^7F_3$ (645 nm), $^7F_4$ (702 nm), and $^7F_5$ (755 nm) ground sub-levels.

The spectral emission of $ZrSiO_4:Sm^{3+}$ TL peaks consists of a number of bands at 565, 605, 660, and 715 nm. These transitions are difficult to assign because the

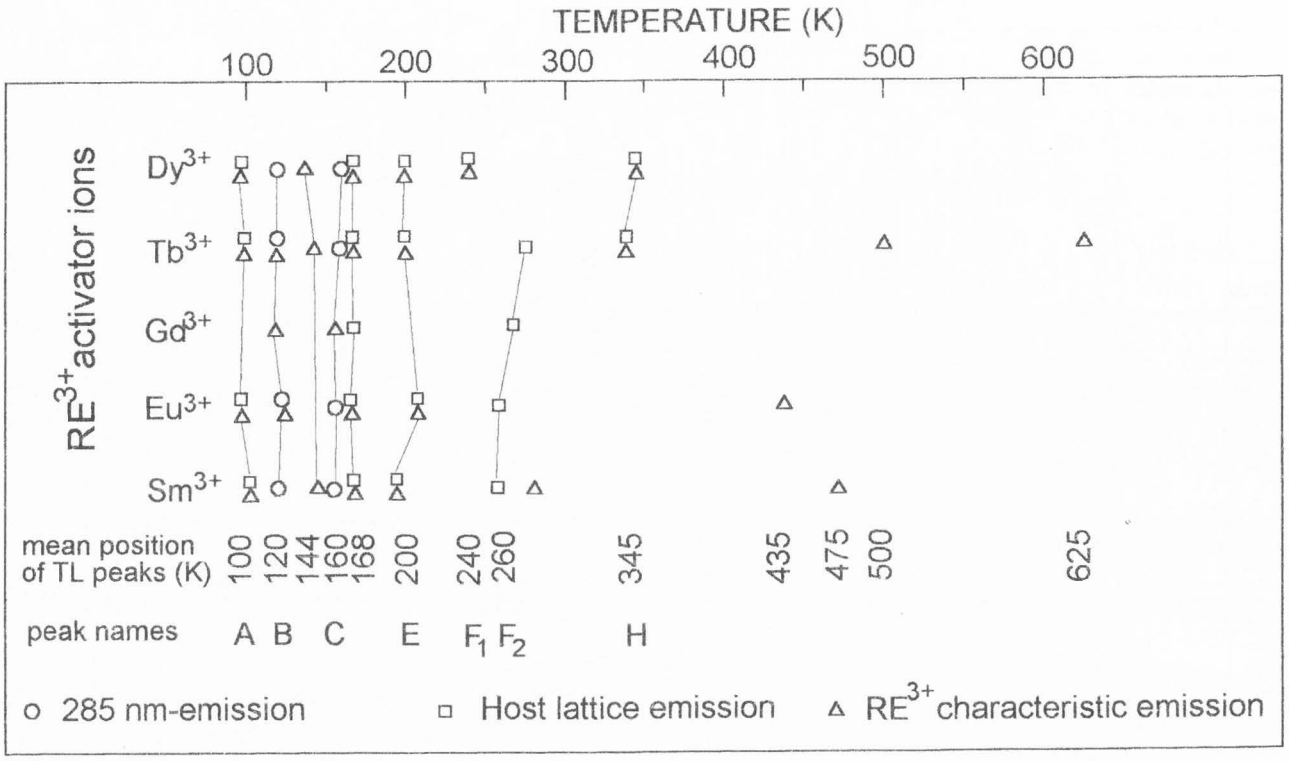

Figure 13. Mean positions of main TL peaks observed in $ZrSiO_4$:RE^{3+} and the three types of emissions which compose them. The peak at 144K is only observed for high RE^{3+} concentrations.

---

interference filter resolution is not great enough. Nevertheless, most of the transition energies between the $^4F_{3/2}$, $^4G_{5/2}$, $^6G_{7/2}$ emitting levels and the $^6H_{13/2, \ldots, 5/2}$ ground state sub-levels agree with the observed values.

In the majority of cases, the characteristic RE^{3+} emissions are associated with the 365 nm emission band (Fig. 13) which has already been described as an host lattice emission (see previous section).

It is well known that the optical excitation of RE^{3+} fluorescence can be governed by one of three possible processes [69]: (1) excitation in the narrow 4f levels of the RE ions; (2) excitation in the broad levels due to 4f-5d transitions or charge transfer mechanisms; or (3) absorption of the host lattice followed by energy transfer from the host lattice to the RE activator.

Moreover, in the case of thermoluminescence phenomenon, the RE^{3+} excitation must be provoked by the detrapping of charge carriers.

It has been shown that Sm^{3+}, Eu^{3+}, Tb^{3+}, or Dy^{3+} excitation is the result of an energy transfer by emission and reabsorption of photons taking place between SiO_4^{4-} host groups and the RE^{3+} emitting centres [43]. This mechanism is ascertained by the fact that Sm^{3+}, Eu^{3+}, Tb^{3+}, and Dy^{3+} characteristic emissions appear at the same temperatures that SiO_4^{4-} emissions and that these RE^{3+} elements can be excited by the host lattice emission (Fig. 14). Recently, Shinno [74] has shown that the luminescence of Dy^{3+} (and also Pr^{3+}, Ho^{3+}, Er^{3+}, and Tm^{3+}) in synthetic doped zircon is excited in the 330-380 nm band and that the characteristic emission of Sm^{3+} or Eu^{3+} element is detected when the doped zircons are excited in the 395-425 nm band. These observations confirm the results reported by various workers who have studied the luminescence of RE^{3+} incorporated in different materials [52, 53, 69]. These authors demonstrate unambiguously that the Dy^{3+}, Tb^{3+}, Eu^{3+}, and Sm^{3+} characteristic emission are excited in the 250-400 nm region.

Fedorovskikh *et al.* [27] observe that the excitation spectrum of Eu^{3+} in zircon contains (besides a series of narrow bands in the region 350-620 nm) a broad band in the region 280-320 nm which they attribute to absorption of the excitation energy of the zircon matrix and its subsequent transfer to the Eu^{3+} ion.

In zircon structure, the lanthanide's replace Zr^{4+} ions (see section **Crystallography**). For materials with zircon structure, Blasse [8] has presented experimental evidence that the transfer due to the energy overlapping is most effective when the central atom of the absorbing group (here SiO_4^{4-}), the intermediate oxide ion and rare earth activator in the host cationic site have a configuration which is as collinear as possible. In the case of zir-

con, the Si^{4+}-O^{2-}-RE^{3+} angles are 149.81° and 99.17°, respectively [72]. If the RE^{3+} and the central ion of absorbing group are not linked to the same ligands (O^{2-} ions), the energy transfer probability becomes very weak. This is the case of the 260K TL peak mechanism, in which an electron is trapped in the vicinity of a Zr^{4+} ion. Effectively, the observed TL emission spectrum of this peak confirms that energy transfer is defective since the only emission really observed is situated at 365 nm.

(b) Energy transfer from OH^- to Gd^{3+} In the case of $ZrSiO_4$:Gd^{3+}, two TL peaks are observed around 120K and 155K. They present an emission peaking at 313 nm and assigned to the $^8P_{7/2} \rightarrow {}^8S_{7/2}$ transition of Gd^{3+} ion. The fact that the characteristic TL peaks of $ZrSiO_4$:Gd^{3+} coincide with the OH^- emission temperatures but not with the host lattice emissions is explained as follows: the excited energy levels of Gd^{3+} are situated at energies higher than the host emission (Fig. 14) and, therefore, the energy transfer described above is not valid for Gd^{3+}. On the other hand, the overlap between the OH^- emission and some Gd^{3+} levels results in the excitation of Gd^{3+} by energy transfer from OH^-.

The RE^{3+} emissions observed at around 120K on TL curves of $ZrSiO_4$:Eu^{3+} and $ZrSiO_4$:Tb^{3+} are related to a similar mechanism of $ZrSiO_4$:Gd^{3+}.

(c) Zircons doped with Sc^{3+}, Y^{3+}, La^{3+}, Ce^{3+}, Pr^{3+}, Nd^{3+}, Ho^{3+}, Er^{3+}, Tm^{3+}, Yb^{3+}, Lu^{3+} These synthetic zircons exhibit TL curves in which any characteristic emission of these individual elements cannot be discerned. The observed curves are either very weak in intensity or similar to the one of undoped zircons. For Sc, La, Ce, Yb, or Lu-doped zircons, there is no doubt: these ions are not TL activators. For the other elements, it is not an absolute certainty. Y^{3+} and Nd^{3+} are well known to emit in the infrared [52], that is out of the spectral range of our equipment. Pr, Ho, Er, and Tm are usually luminescent when they are excited in the 330-380 nm range [52]. According to our energy transfer model, it should be possible to observe their characteristic emissions which are expected in visible [52]. Owing to the poor resolution of the interferential filters used and since the main transitions of these trivalent elements are closed to the ones of Dy^{3+} (or Tb^{3+}) which pollutes our samples, we are not able to detect any luminescence clearly due to these elements. However, a weak emission observed at 520 nm from Z_F:Er^{3+} could be due to the $^2H_{11/2} \rightarrow {}^4H_{15/2}$ transition of Er^{3+}.

T > 350K temperature range In synthetic zircons, some TL peaks have been observed for temperatures higher than 350K. It is a question of the 435K peak of $ZrSiO_4$:Eu^{3+}, the 500K and 625K peaks of $ZrSiO_4$:Tb^{3+} and of the 475K peak of $ZrSiO_4$:Sm^{3+} of

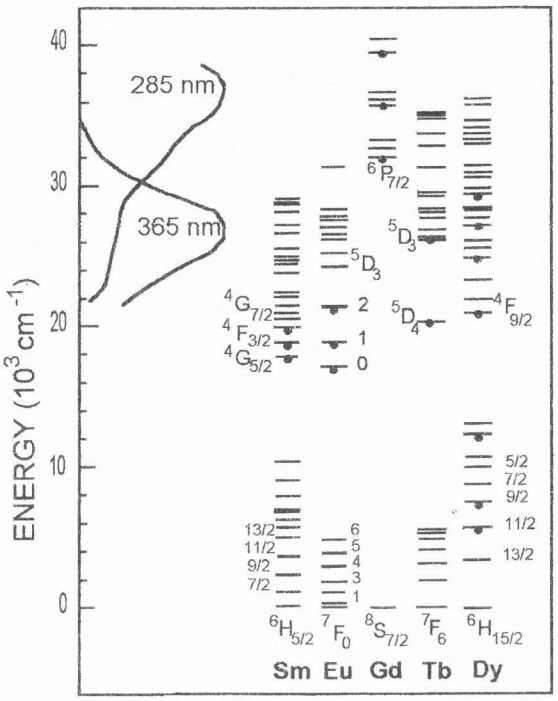

Figure 14. Energy levels of Dy^{3+}, Tb^{3+}, Gd^{3+}, Eu^{3+}, and Sm^{3+} ions as given by Dieke [20] and overlapping of some of them by host lattice or OH^- emission.

---

which the spectral emission is only constituted by the RE^{3+} characteristic emission. The latter is only seen after UV-254 nm excitation. In these cases, the energy transfer mechanism is not available because there is no host lattice emission at these temperatures. On the other hand, these TL peaks are probably the result of charge transfer mechanisms related to the RE^{3+} which transform into Sm^{2+}, Eu^{2+} or Tb^{4+} upon radiation.

Owing to their electronic structures, Dy^{3+}, Tb^{3+}, Eu^{3+}, and Sm^{3+} do not have the same behaviour. In the lanthanide transition group, they are situated on both sides of Gd^{3+} which is relatively stable because of its configuration $4f^7$. $Tb^{3+}(4f^8)$ has a tendency to release a 4f-electron (to trap a hole) and then to become $Tb^{4+}(4f^7)$, whereas, $Eu^{3+}(4f^6)$ tends to appropriate an electron of the neighbouring anions to become $Eu^{2+}(4f^7)$. The two mechanisms, $4f^8 \rightarrow 4f^7 5d$ transition for Tb^{3+} and charge transfer for Eu^{3+}, require little energy.

Furthermore, Blasse [9] has argued that, in oxygen-containing host lattices, two types of transitions can be distinguished: a charge transfer transition from ligands (usually O^{2-} ions) to central RE ion, and intraionic $4f \rightarrow 5d$ transitions. The former will be found for RE ions that are easy to reduce (Eu^{3+}, Sm^{3+}); the latter is more common for RE ions that are easy to oxidise (Tb^{3+}).

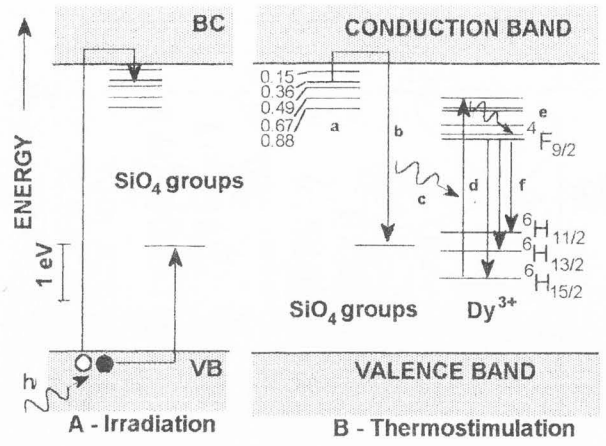

Figure 15. Energy level diagram describing the process of TL in zircon from 77K to 350K.

(A). Irradiation. Production and trapping of electrons and holes. The electron traps are localised in the vicinity of Si^{4+} or Zr^{4+} ions whereas the holes are trapped by oxygen ions. The band gap of zircon has been estimated at about 5.4 eV from optical absorption measurements [29].

(B). Heating. (a) Thermal detrapping of electrons trapped in Si-O system (SiO_4^{4-} group). (b) Radiative recombination of the released electrons on the oxygen sites with 365 nm-emission (host lattice emission). (c) The host lattice emission band and the absorption transitions of the RE^{3+} ion (here Dy^{3+}) overlapping each other, there is an energy transfer by emission-reabsorption mechanism from host lattice to RE^{3+} ions. The part of non-reabsorbed 365 nm-emission is emitted. (d) Excitation of RE^{3+} ions. (e) Radiationless transitions from the absorption level to the emitter level (here $^4F_{9/2}$). (f) Radiative transitions from the emitter level ($^4F_{9/2}$) to the ground sub-levels of RE^{3+} (here $^6H_{11/2, 13/2, 15/2}$) with characteristic emission of RE^{3+}.

In this way, Tb^{3+} and Eu^{3+} ions can be act as traps for holes and electrons, respectively. Because of their high stability, the activation energies required for the charge carriers detrapping might be relatively high.

So, the observed TL peaks are probably related to the following schemes:

$ZrSiO_4$:Eu^{3+} (or Sm^{3+}) irradiation:

$$Eu^{3+} + e^- \rightarrow Eu^{2+} \text{ (trapped electron)}$$

$ZrSiO_4$:Eu^{3+} heating at 435K:

$$Eu^{2+} \rightarrow (Eu^{3+})^* + e^- \rightarrow$$
$$Eu^{3+} + h\nu_{Eu} + \text{released electron}$$

$ZrSiO_4$:Tb^{3+} irradiation:

$$Tb^{3+} + e^+ \rightarrow Tb^{4+} \text{ (trapped hole)}$$

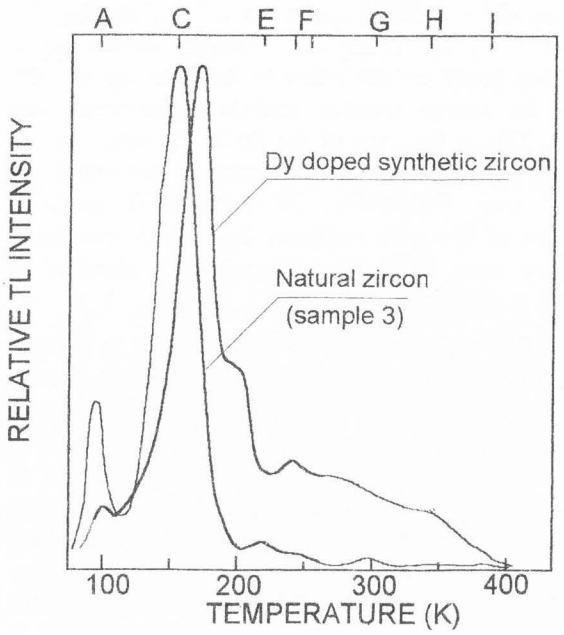

Figure 16. Comparison between the TL curves obtained from a natural (sample 3) and a synthetic Dy-doped zircon after X-irradiation at LNT [40]. The letters indicate the typical positions of TL peaks.

$ZrSiO_4$:Tb^{3+} heating at 500 then 625K:

$$Tb^{4+} \rightarrow (Tb^{3+})^* + e^+ \rightarrow Tb^{3+} + h\nu_{Tb} + \text{released hole}$$

Tb^{4+} [7, 37] and Eu^{2+} [25] have been observed in zircon. According to the EPR results of Bershov [7], it is probable that the hole trapped by Tb^{3+} originates from the nearest oxygen sites. The presence of two oxygen ions at different distances from terbium causes the appearance of the two physically different EPR spectra observed by Bershov in natural zircon [7]. In this case, the activation energies required for destroying the two complexes formed by Tb^{4+} replacing Zr^{4+} correspond to 375K-425K and 575K-625K, respectively [7]; these values agree fairly well with our measurements in TL of synthetic zircon (500K and 625K, respectively).

$ZrSiO_4$:Eu^{2+}, Eu^{3+} has been obtained by calcination of synthetic $ZrSiO_4$:Eu^{3+} in hydrogen [25]. Bivalent europium is responsible for a broad band having a maximum at 450-460 nm.

Conclusion

Depending on the temperature range, two model types are available for interpret the TL of synthetic zircons. In the 77-350K range, the various steps occurring are summarised in Figure 15; this model involves energy transfer processes from the host lattice emission (HLE) to the RE^{3+} ions. At temperatures higher than 350K, the trapping and luminescence mechanisms are related to charge conversion mechanisms.

Table 2. TL properties of unannealed natural zircons observed after irradiation at LNT or RT from 20 and 12 samples, respectively. T(K): mean values and standard deviation observed on TL peak temperatures; %: occurrence frequencies; OH: OH^- emission; HLE: host lattice emission; Dy: Dy^{3+} emission; Dy+Tb: Dy^{3+} and Tb^{3+} emissions are simultaneously present; Dy(Tb): the Tb^{3+} emission can occasionally replace the Dy^{3+} emission. After ([44], [14]).

	TL peak positions and frequency occurrence						Luminescent centres		
TL peak	LNT irradiation		RT irradiation				OH	HLE	RE
	[44]		[44]		[47]	[49]	[44]		
	T(K)	%	T(K)	%	T(K)	T(K)			
A	97 ± 1	80					x	o	Dy
B	116 ± 5	20					?		
C	155 ± 4	100					x	o	Dy(Tb)
D	181 ± 2	20						o	Dy
E	219± 3	45							Dy(Tb)
F	240± 3	75							
F	267 ± 6								
G	301 ± 6	65							Dy
H	343 ± 5	65	343 ± 2	92		345		o	Dy
I	378 ± 7	75	379 ± 3	92	373	382		o	Dy
J			458 ± 10	58	453	468			Dy
K			518 ± 4	58	503	501			Dy
						518			
L			566 ± 7	58	548	541			
						582			
M			610 ± 5	26	638	623			Dy+Tb
N			658 ± 5	17	673	655			

In order to explain the RE^{3+} cathodoluminescence excitation mechanism, two models are used. Yang *et al.* [105] suppose that the energy transfer model apply to zircon except that the recombination electrons are not thermally released but are released from Si^{3+} ions by the incident high-energy electron beam. Fedorovskikh *et al.* [26] suggest that during cathodic excitation, both radiative and non-radiative energy transfer from the matrix to the RE^{3+} activator are possible. On the other hand, Remond *et al.* [70] think that the excitation process is rather consistent with a charge conversion model.

Thermoluminescence of Natural Zircons

Peak temperature positions

The TL properties of natural zircons from various origins have been systematically studied after X-irradiation at LNT or RT [44] (Table 2). The so-called "C" peak, situated at 155K ± 4K is always present and, in any case, is found to be the main TL peak (Fig. 16). The TL curves obtained after UV (254 nm), X- (45 kV), γ (^{137}Cs), or β- (^{90}Sr) irradiation at RT are similar [45]. Most of studied zircons exhibit TL curves analogous to one or the other curves reported in Figure 17 [38]. Peaks A, E, F, G, H, I, J, K, and L occur frequently (>> 45%). These TL peak temperatures are in good agreement with the results of Shulg'in *et al.* [75] and the H, I, .., N ones agree fairly well with those of other workers [47, 49].

TL emission centres

The OH^-, Dy^{3+} and host lattice emissions described

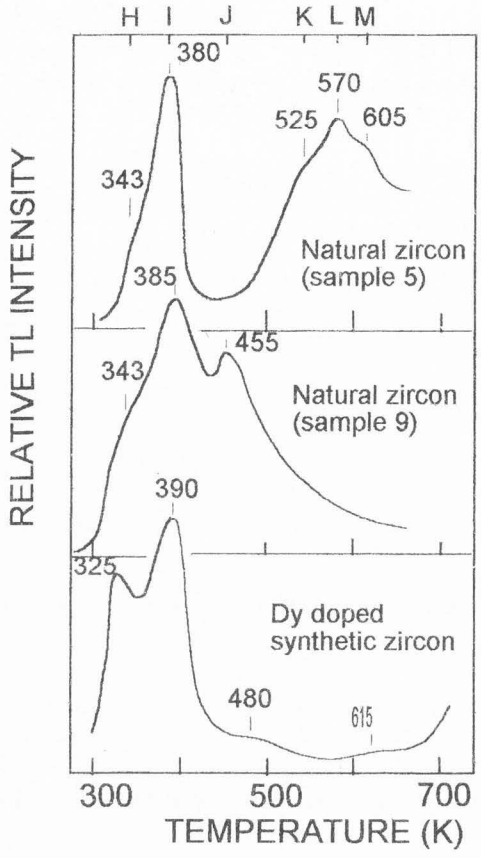

Figure 17. The two kinds of TL curves observed after irradiation at RT from natural zircons [38]. Comparison with the TL curve of Dy doped synthetic zircon obtained in the same conditions.

---

in the previous section are identified in the TL peak emission spectra of natural zircons. These three emissions occur simultaneously in the peaks A and C (Fig. 18). The host lattice emission associated with that of Dy^{3+} is observed in peaks D, H, and I. Finally, the peaks E (Fig. 19), G, J, K, and M are only constituted by the Dy^{3+} emission; sometimes, a very weak host lattice emission is associated with these peaks. The Tb^{3+} characteristic emission is irregularly observed for specific TL peaks. In some cases, it is associated with the Dy^{3+} emission (Fig. 20), while in other cases, it is by itself [48]. After 258 nm-UV excitation at RT, we have also observed, occasionally and for certain TL peaks, the appearance of the Sm^{3+} emission [38, 45]. For the same sample, this emission was not detected after X-irradiation.

These observations are in good agreement with the data found in the literature which confirms that Dy^{3+} is a common TL activator in natural zircon and that is sometimes associated to the HLE.

The spectra of natural zircon contain a feature near

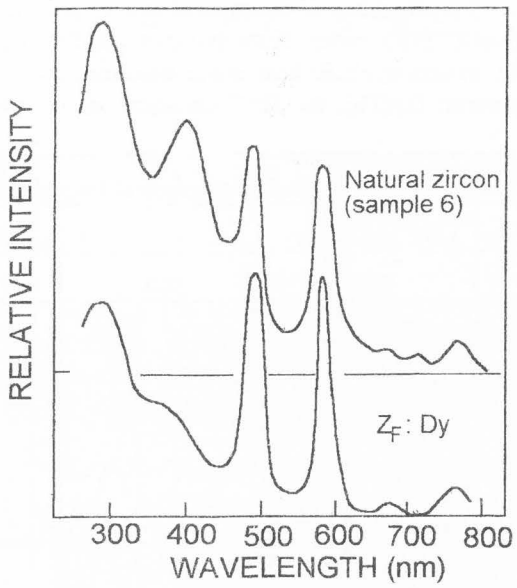

Figure 18. Emission spectra of TL peak C obtained after X-irradiation at LNT from an unannealed natural zircon (sample 6) and from an hydroxylated synthetic Dy^{3+} doped zircon Z_F: Dy [44].

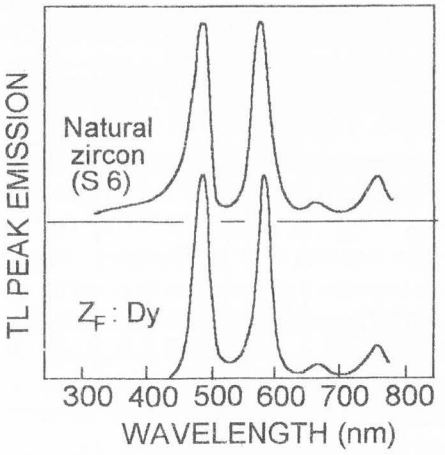

Figure 19. Emission spectra of TL peak E (220K) obtained after X-irradiation at LNT from an unannealed natural zircon (sample 6) and from an hydroxylated synthetic Dy-doped zircon [44].

---

385 nm which is a broad luminescence band clearly apparent for the 350K (peak H) and 382K (peak I) but very weak at higher temperatures [16, 48, 49].

Zircon samples show the strong line features characteristic of Dy^{3+} for the TL peak I (373K) but at higher temperature lines assigned to Tb^{3+}, and in some cases to Eu^{3+}, are resolved [16]. Jain [48] observes that the peaks at 453K and 548K (peaks J and L, respectively) found in the TL of sand samples exhibit the Tb^{3+} emission associated or not with the host lattice emission.

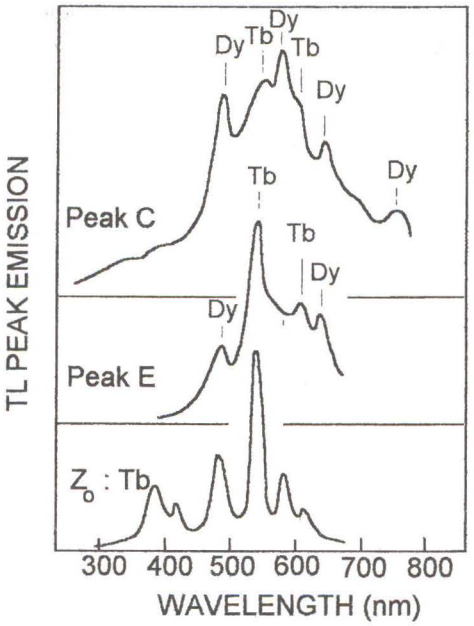

Figure 20. Emission spectra of TL peaks C and E obtained after X-irradiation at LNT from a natural zircon (sample 7). Comparison with the TL emission spectrum of synthetic Tb-doped zircon [44].

In synthetic zircons, we have shown that Dy^{3+}, Tb^{3+}, Gd^{3+}, Eu^{3+} and Sm^{3+} are activators of TL but, in this case, these elements were introduced individually into the zircon lattice. It is not the same situation which occurs in natural zircon where all trivalent rare earth's and other impurities are simultaneously present [32, 79]. In this latter case, we clearly demonstrated that Dy^{3+} is the principal activator of the natural zircon [44].

In considering the processes involved, three potential causes can be suggested to explain the constant presence of Dy^{3+} emission: **(1)** In natural zircon, Dy has the higher concentration. The relative abundance of the concerned RE is Dy > Gd > Tb = Eu > Sm [65, 79]. **(2)** Because of a different oscillator strength for the same concentration of different RE^{3+}, the relative intensity of their luminescence spectra is dissimilar [55]. For instance, the relative intensities of various RE^{3+} in two crystals is given (Table 3). **(3)** The energy transfer probability is better for Dy than for the other RE. At higher temperatures, other RE are seen because there is a charge conversion mechanism.

Trapping centres and related mechanisms

(a) TL peaks A, C, E, F, and H Table 2 shows clearly that the positions of natural zircon TL peaks situated below 350K agree fairly well with the positions of synthetic zircon TL peaks. It is the same for the emission spectra of these peaks. In most cases, the trap luminescence centres related to these peaks have been identified and described in the previous section. Thus, the trapping centres related to peaks A, C, E, F, and H are associated with the SiO_4^{4-} groups. In this case, the electron-hole recombination takes place with an emission band situated between 380 and 400 nm (instead of 365 nm in synthetic zircon). A part of the host lattice emission can be absorbed by Dy^{3+} (or some other RE^{3+}) centres, which are included in the natural zircons, and used to excite the characteristic emission of the ones. The emission spectrum of Dy^{3+} consists of narrow lines in the region around 480, 580, 662, and 760 nm and, generally, is simultaneously observed with the host lattice emission. On the contrary, the HLE is not observed in the emission spectrum of some TL peaks (i.e., peak E, Fig. 19). This could signify that the energy transfer is complete; it agrees with the results of Fedorovskikh *et al.* [26] who report that the probability of energy transfer is decreased as the temperature is reduced.

Table 3. Repartition of relative intensities of Dy^{3+}, Tb^{3+}, Gd^{3+}, Eu^{3+}, and Sm^{3+} luminescence spectra observed in Y_2O_3 and La_2O_3 compounds. After Marfunin [55].

	Dy^{3+}	Tb^{3+}	Gd^{3+}	Eu^{3+}	Sm^{3+}
Y_2O_3	100	60	5	50	5
La_2O_3	3	180	2	5	1

The OH^- mechanism is responsible for the most energetic part of the emission occurring in the peaks A and C (Fig. 17). The temperature of the first OH^- emission (97K ± 1K) has not been observed in synthetic samples but it is possible that the recombination of electrons released by traps A takes place with some OH^- previously generated by X-irradiation at 77K (see the section **Contribution of OH^- ion**). In this case, the OH^- emission of both peaks A and C would be related to the same OH + e^- recombination process while the peak B (116K) would correspond to the recombination of O^- and H^o as explained in the previous section. There is no evidence for this latter assumption because it is not possible to record the emission spectrum of the TL peak B which is very weak.

Kirsh and Townsend [49], argue that the characteristic emissions of Dy^{3+} and the host lattice, relative to TL peak H registered after irradiation at room temperature, do not appear at the same temperature (Table 4). They explain the Dy^{3+} emission by a charge conversion mechanism. They interpret that during X-irradiation at RT, some of the Dy^{3+} ions are reduced to Dy^{2+} by electron capture and holes are trapped at various unidentified centres. When the temperature is raised, the holes are released and the recombination occurs at the Dy sites with the characteristic emission of Dy^{3+} whereas the

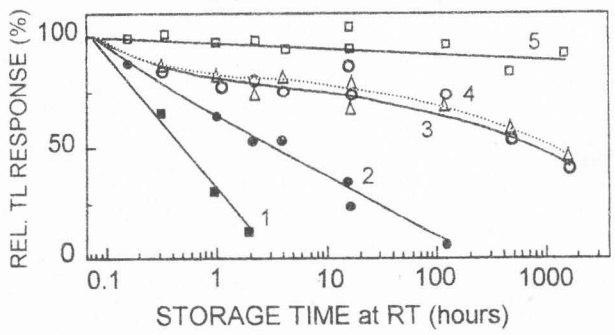

Figure 21. Fading of zircon TL emissions occurring at: (1) 325K, 480 nm; (2) 350K, 345 and 480 nm; (3) 385K, 480 nm; (4) 385K, 345 nm; and (5) 600K, 545 nm; after storage at RT.

Table 4. Parameters of the TL peaks H and I recorded by Kirsh and Townsend [49] at wavelengths longer than 450 nm (Dy) and at 385 nm (HLE: host lattice emission) after X-irradiation at RT. Comparison with the parameters measured, by the initial rise method, for the 480 nm emission (Dy) and for the 365 nm emission (HLE) after X-irradiation at RT (this work). T: peak temperature; E: trap depth; s: frequency factor.

		After [49]			This work	
peak	Emis.	T(K)	E(eV)	s(Hz)	T(K)	E(eV)
	Dy	345	0.82	$2.4.10^{10}$	323	0.89 ± 0.07
H	HLE	350	0.89	$1.6.10^{11}$	350	1.13 ± 0.05
	Dy	382	1.18	$1.1.10^{14}$	383	1.20 ± 0.06
I	HLE	382	1.18	$1.1.10^{14}$	383	1.27 ± 0.06

host lattice emission appears as described before. We have effectively observed that the two emissions (host lattice and Dy^{3+}) obtained after X-irradiation at RT do not coincide (Table 4). In fact, it seems that the TL peak at 350K is constituted by both emissions, the HLE being predominant while the TL peak at 325K exhibits only Dy^{3+} emission; it is difficult to resolve these two peaks since they are very close. Figure 21, which shows that the two components of the TL peak 350K fade at the same rate, confirms this result.

(b) TL peaks D, G, I, J, K, L, ... The comparison with the synthetic zircon TL does not permit us to explain the TL mechanisms governing the peaks D, G, I, J, K, L, ..., which do not exist in synthetic samples (Figs. 16 and 17); but, it is possible that, in natural zircons, the various and numerous impurities generate several types of defects able to trap electrons extracted from silicate group's oxygen ions.

As shown in section **Influence of trivalent rare earth impurities**, the presence of RE^{3+} characteristic emissions unaccompanied by the host lattice emission in the high temperature TL peaks can be explained by charge conversion mechanisms. In the same way, several TL peaks with activation energies between 0.82 and 1.60 eV, and typical emission spectra of Dy^{3+}, are attributed to RE^{3+}-hole recombination [49]. The 382K peak (peak I) which displays both the 385 nm band and the Dy^{3+} lines, might be associated with an electron captured by a Dy^{3+} ion and a hole trapped at an adjacent lattice O^{2-}, the recombination of which excites both the SiO_4^{4-} groups and the RE ions [49].

Radiation Damage in Natural Zircons

The metamict state

Among the various impurities which are found in natural zircons, U and Th (and their daughter products 238U, 235U, and 232Th decay series) are radioactive. It is now well established that the radioactive decay of these radio nuclides causes accumulated structural damages which can lead to a complete destruction of initially well-crystallised zircons. This phenomenon, which takes place throughout the geologic history of zircons, is called metamictisation. Although the total radiation dose consists of contribution from α and β particles, γ-rays, recoil nuclei, and the products of spontaneous fission, it is expected that α particles and recoil nuclei are chiefly responsible for the radiation damages [34, 35]. In the first occurrence, the damage is caused by two simultaneous processes associated with the α-decay event [23]: (1) An α particle ($\sim$ 4.5 MeV) with a range of 10 μm dissipates most of its energy by ionisation and displaces several hundred atoms creating Frenkel defect pairs. (2) The α-recoil atom ($\sim$ 0.07 MeV) with a range of 10 nm produces several thousand atomic displacement creating tracks of disordered materials. These two damaged areas are separated by thousands of unit cell distances and are expected to have different effects on the crystalline structure [23].

Holland and Gottfried [35] have shown that the refractive index and the density of zircons decrease from 4.7 to 3.9, while the unit cell dimensions increase, with increased total α-dose absorbed by the zircons. The unit cell parameters a_0 and c_0 increase respectively from 0.660 to 0.670 nm and from 0.598 to 0.609 nm with absorbed α-doses increasing from 0 to $0.41 \cdot 10^{16}$ α-decay events/mg. For α-dose higher than $0.41 \cdot 10^{16}$ α-decay events/mg the parameters remain unchanged. Holland and Gottfried [35] have also shown, with Hurley and Fairbairn [36] that structural defects cause diffuse lines of X-ray diffraction photographs, decrease the intensity of the lines and, when the radiation reaches

$6 \cdot 10^{15}$ α-decay events/mg, cause the disappearance of the lines.

The breakdown of the structure is envisaged as a four-stage process in which the structure is first saturated with displacements, then the saturated structure breaks down into crystallites of ordered zircon which ultimately break down into a glass [35].

In the model developed by Pellas [68], the crystal structure of zircon is broken down into four phases during the process of metamictisation. These four phases are primarily an expanded zircon phase which contains a high concentration of interstitials and vacancies. Continued radiation damage finally results in a break up of the zircon lattice into ZrO_2, SiO_2 and amorphous zircon.

Bursill and McLaren [11] have argued that the simplest defects expected to be generated by the internal radiation are isolated vacancies and interstitials, but the electron microscope they used was not able to resolve these defects. However, these authors could detect the presence of crystalline ZrO_2 in some metamict zircons. The Pellas' model is also confirmed by Wasilewski *et al.* [97] who think that, in the first stage, the primary damage is the production of interstitial atoms which cause deformation of the isolated SiO_4 tetrahedron, and by Vance *et al.* [89], who have shown that the principal defect in radiation damaged zircon is the displaced oxygen ion. On the other hand, no evidence of SiO_2 or ZrO_2 has been found in radiation damaged zircons [4, 24, 34, 87, 103]; some have concluded that the end product seems to be a glass rather than a mixture of SiO_2 and ZrO_2 [34, 87, 103].

Headley *et al.* [33] have shown that metamict zircon possesses two distinct structures, one interpreted as amorphous and the other as being composed of slightly misoriented microcrystallites. Finally, the investigations of Yada *et al.* [103, 104] show that metamictisation proceeds principally by the formation of fission tracks, directly resulting from the fast movement of nuclear particles; recoil nuclei from them seems to play a less important role in the destruction of structure.

According to Murakami's group [17, 58, 59], three stages of damage accumulation may be delineated. In stage I ($< 3 \cdot 10^{15}$ α-decay events/mg), damage is dominated by the accumulation of isolated points defects which cause unit-cell expansion and distortion which accounts for most of the decrease in density. In stage II ($3 \cdot 10^{15}$ - $8 \cdot 10^{15}$ α-decay events/mg), microstructure consists of distorted crystalline regions and amorphous "tracks" caused by α-recoil nuclei. Stage III ($> 8 \cdot 10^{15}$ α-decay events/mg) consists of material that is entirely aperiodic as far as it can be determined by X-ray or electron diffraction.

The Pellas' model [68] seems unlikely in view of the recent X-ray spectroscopic studies of Farges and Calas [24]. The major changes observed during the metamictisation of zircon correspond to a co-ordination change around Zr which is reduced from 8 to 7 and to a regular significant decrease of Zr-O distance. These two observations would imply the creation of oxygen vacancy in the ZrO_n polyhedron and tilting of the SiO_4 tetrahedra. The model of metamictisation proposed by Farges and Calas [24] is confirmed by Woodhead *et al.* [101] and by Mursic *et al.* [61].

Various workers have noticed the role played by OH and H_2O in the metamict state stabilisation by local compensation of charge [1, 15]. Following Woodhead *et al.* [101], hydrous components enter the structure only after the total metamictisation, but the amounts are not correlated with U-Th contents. In all cases, OH is the only hydrous species detected; it is present only in metamict or nearly metamict samples [101].

An important field of research is the comparison of radiation damage effects in artificially irradiated synthetic zircon with those in natural zircon. The amorphisation dose depends on the irradiation temperature, the energy and the mass of used particles [96]. It increases with temperature in two stages (below 300K and above 473K) and is nearly independent of the damage source (α-decay events or heavy ion beams) at RT [99]. A dosage of about 10^{16} fission events/cm^3 appears to be required to render a zircon amorphous [88]. For ion implantation, the transition from the crystalline to the metamict state occurs in the range of 10^{13} to 10^{15} ions/cm^2 [12, 34, 59]. The study of damaged accumulation process in Pu-doped zircons shows that the amorphous state is reached at $6.7 \cdot 10^{15}$ α-decay events/mg [98].

Recrystallisation of damaged zircons

The results of tests made on the annealing of partially metamict zircons at elevated temperatures by Hurley and Fairbairn [36] confirm those described by Pabst [66]. It is found that, if a crystal is not greatly disordered, it would return to a degree of order very close to that of a perfect crystal. According to Kulp *et al.* [51], the recrystallisation of metamict zircons takes place at temperature from 1160K to 1180K. Frondel and Collette [30] have found that, when heated in water vapour, metamict zircons recrystallise at temperatures below these needed for recrystallisation in dry air. This fact is confirmed by Bursill and McLaren [11]. Recrystallisation of metamict zircons is attested by IR spectra [40, 87, 97], by X-ray diffraction [36], by restoration of the density, refractive index values [86], and TL intensity [14, 44, 62, 91]. The physical property recovery of very metamict samples is incomplete and suggests that greater the damage less is the recovery [97].

Mursic *et al.* [60] show that zircon crystallisation by heating up from the metamict state is promoted via a

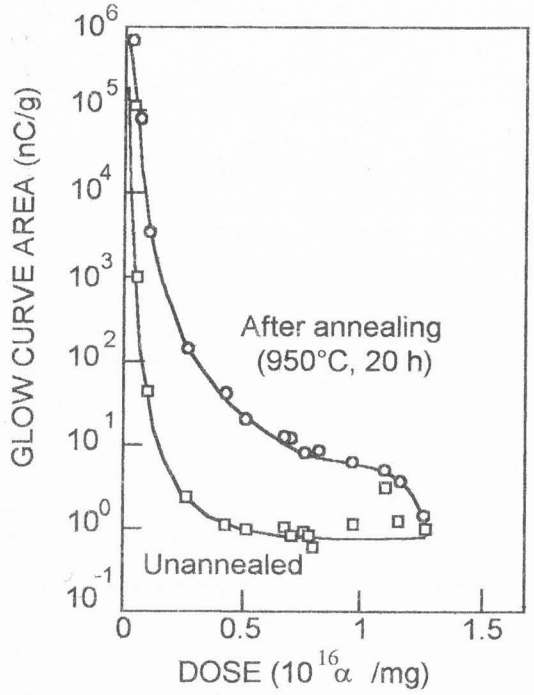

Figure 22. Integrated glow-curve area of Ceylon zircons after irradiation with γ-rays as a function of the total α-dose of the sample as given by Vaz and Sentfle [90]. One set of measurements is obtained from the unannealed samples, the other after they have been heated at 1225K for 20 hours.

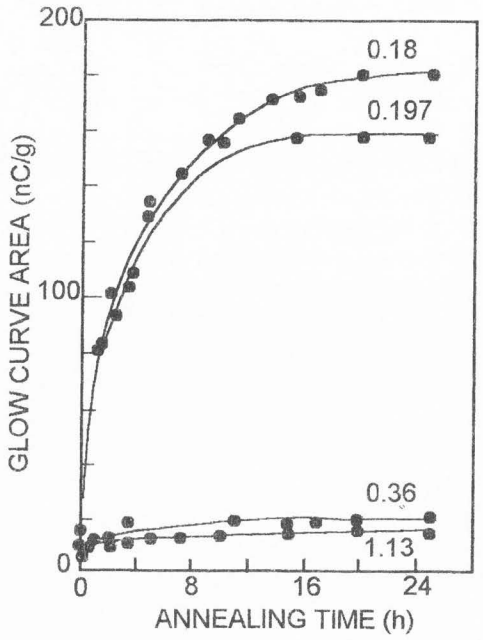

Figure 23. Integrated glow-curve area of Ceylon zircons with different α-doses (expressed in 10^{16} α-decay events/mg) as a function of annealing time at 1225K as given by Vaz and Sentfle [91]. The samples have been irradiated with the same γ-rays exposition before each TL readout.

---

rearrangement of the Zr-O subunit, whereas, Weber *et al.* [99] show that it occurs above 1300K and is a two-step process that involves the initial formation of pseudo-cubic ZrO_2.

Thermoluminescence of partially metamict zircons

Krasnobaev [50] finds that the natural TL output of zircons from different localities is a function of the total α-dose they have absorbed. Vaz and Senftle [91] show that the γ-ray induced TL of damaged zircons decreases rapidly with the α-dose (Fig. 22). At an α-dose of about $0.25 \cdot 10^{16}$ α-decay events/mg, the TL output of these unheated samples is reduced by 10^5. At greater α-doses, the TL emission of the samples shows no significant change. Vaz and Senftle [91] also find that the restoration of TL output after the sample has been annealed (1225K, 20 hours) is dependent of α-dose (Fig. 22). The magnitude of the change in TL output, as well as its maximum intensity depends both on the annealing time and the a dose received by the samples (Fig. 23). The results of Vaz and Sentfle [91] have been confirmed by other workers [14, 44, 62].

We have investigated the correlation between the TL peak C intensity presented by natural zircons and their unit cell volumes [44]. According to the Figure 24, the unannealed zircons can be classified into two families: the "normal" zircons, characterised by an unit cell volume V_o and a TL intensity higher than I_o, and the radiation damaged zircons, with unit cell volumes V greater than V_o and TL intensities I lower than I_o. The unit cell volume values characterise the metamictisation degree of zircons. Following the data of Holland and Gottfried [35], the unit cell volume of well-crystallised zircons is $V_o \approx 0.261$ nm^3. By absorption of about $0.4 \cdot 10^{16}$ α-decay events/mg, the unit cell volume become $V \approx 0.274$ nm^3. For α-doses greater than $0.4 \cdot 10^{16}$ α-decay events/mg, V remains equal to 0.274 nm^3 [35]. In examination of Figure 24, it must be borne in mind that the TL intensity is disturbed not only by the metamictisation phenomenon but also by the impurity concentration. However, Vaz and Sentfle [91] have noticed that the influence of the latter on the TL intensity is less than the metamictisation process. The very important dispersion of the unit cell volume observed for some zircons (such as sample 10 or 11, Fig. 24) is the result of the inhomogeneity of the crystal. The optical microscope investigation of these samples reveals the existence of a metamict core surrounded by a better crystallised region.

Thus, the TL appears to be a method very sensitive to characterise very low degrees of metamictisation [22]. The TL intensity varies by several orders of magnitude

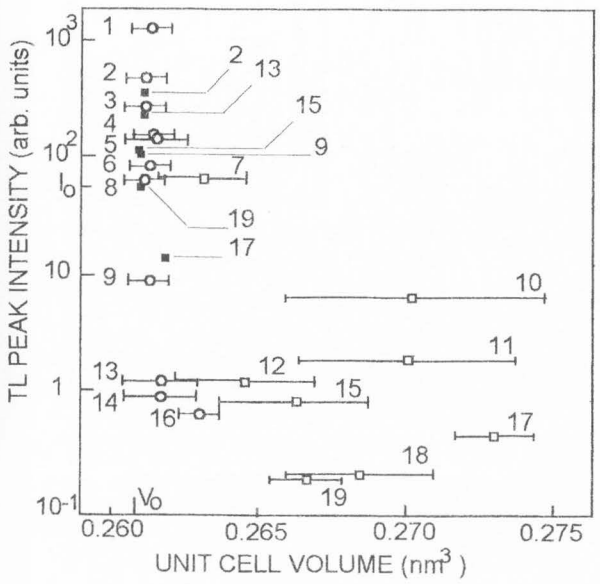

Figure 24. Correlation between the TL intensity of peak C and the unit cell volume of the studied sample. Circles: unannealed non-metamict zircons; hollow squares: unannealed semi-metamict zircons; solid squares: annealed zircons. The numbers refer to the sample designation. The physical description and the origin of the various natural zircons are given in [44]. V_o is the unit cell volume value of well crystallised zircons, I_o is the threshold value of TL peak C intensity (see text).

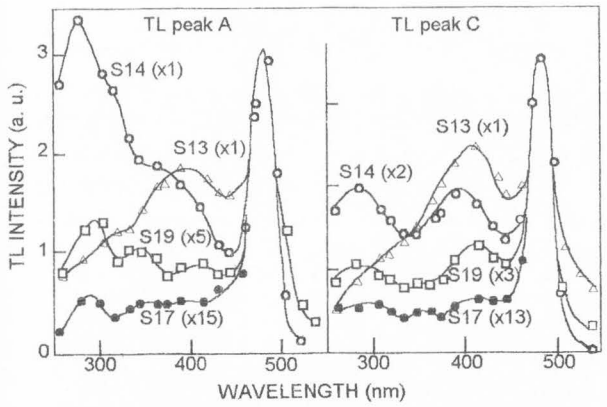

Figure 25. TL emission spectra of peaks A and C obtained after X-irradiation at 77K from samples 13, 14, 17, and 19. Only sample 13 presents no metamict character [44]. The three kinds of emission are observed: OH^- (285 nm), HLE (400 nm), and Dy^{3+} (480 nm).

---

and is inversely correlated with the metamictisation degree of zircon [14].

After annealing (1270K, 24 hours), all the damaged zircons, except sample 17, have found again their original values ($I > I_o$, $V = V_o$). The behaviour of sample 17, which is very metamict, confirms the observations of Wasilewski *et al.* [97] who find that greater is the initial degree of radiation damage, more difficult is to reorganise the lattice by a given heat treatment.

As a general rule, the effect of annealing is to rearrange the TL peak positions and to decrease their dispersion. In example, the mean temperatures of TL peaks F_2 and H obtained, before and after annealing of six samples, shift from 273K ± 10K to 266K ± 3K and from 339K ± 5K to 346K ± 1K, respectively [44].

Examples of TL peak emission spectra of high density zircons ("normal" zircons) are given in Figures 18, 19, and 20. Because of their weak intensities, it is difficult to analyse the low temperature TL peak responses of very metamict zircons, but after annealing, the determination becomes possible. The TL peak emission spectra of annealed damaged zircons are identical to those of well crystallised samples [40]. Particularly, they present OH^- specific emission bands at 95K and 154K (Fig. 25). This result must be compared to that obtained in the case of the hydroxylated synthetic zircon Z_F annealing in which the OH^- emission band intensities have been strongly reduced (section on **Synthetic Zircon**). The presence of OH^- emission in all the studied samples is in contradiction with the work of Woodhead *et al.* [101]. These authors have shown that the samples with a event decays below $\approx 4 \cdot 10^{15}$ α/mg do not contain OH or H_2O while all those with higher U contents contain OH.

After X-irradiation at RT, the spectral study of some unannealed metamict zircons is possible. In this way, we can follow the evolution of TL peak emission spectra due to annealing (Fig. 26). Before annealing, the emission spectra of TL peak H consist of a broad band centred around 600 nm and situated around 345K. The annealing causes the disappearance of this emission and gives rise to a TL peak around 325K with a Dy^{3+} characteristic emission (Fig. 27). The peak which appears after annealing around 385K behaves in the same way. Its emission spectrum consists of characteristic Dy^{3+} transitions associated with the host lattice emission (Fig. 28). This peak replaces the TL peaks first located, before annealing, at 398K or 435K. A similar behaviour is observed for higher TL peaks occurring in some samples (Fig. 29).

The broad band centred around 600 nm arises in fluorescence spectrum obtained under UV light and has been related to luminescent centres produced by the radioactive decay of the U and Th present in zircon lattice [63]. Such an emission has also been observed in UV induced TL peaks of unannealed natural zircons and vanishes when they are strongly heated [38].

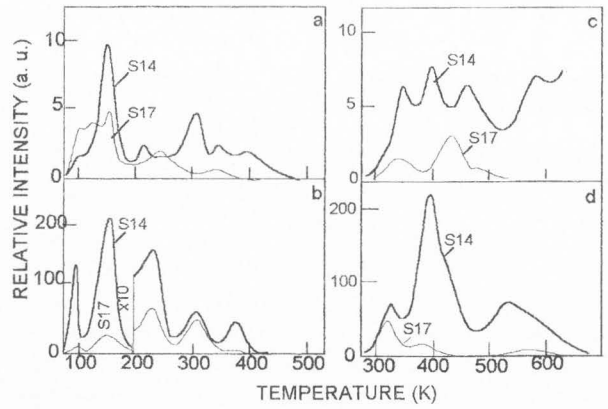

Figure 26. TL curves recorded from samples 14 and 17, after X-irradiation at LNT: (a) before annealing and (b) after annealing at 1275K, 24 hours, in air; and after X-irradiation at RT: (c) before annealing and (d) after annealing in the same conditions.

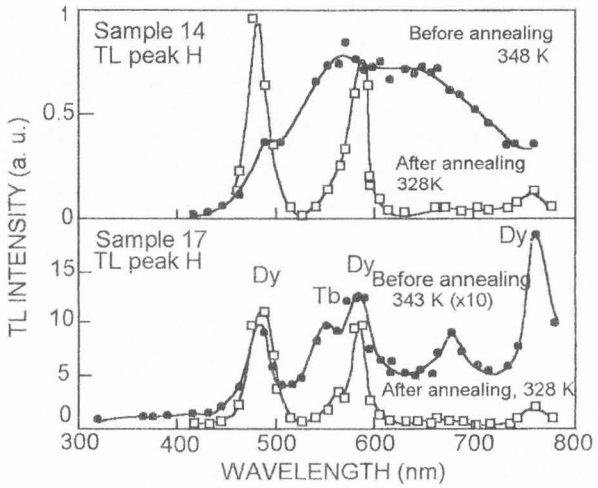

Figure 27. Emission spectra of TL peak H obtained after X-irradiation at RT from two semi-metamict zircons (samples 14 and 17) before and after annealing at 1275K, 24 hours, in air.

The rearrangement of the peak positions and the disappearance of the broad 600 nm-band can be considered as a proof of the host lattice reorganisation which results in a restoration of normal zircon.

TL dating methods

The use of TL for dating archaeological ceramics is well established [2, 80]. The TL dating of archaeological (and geological) samples consists essentially of two basic steps, the determination of the natural dose which a sample has absorbed during its past and the determination of the corresponding natural dose. From these two

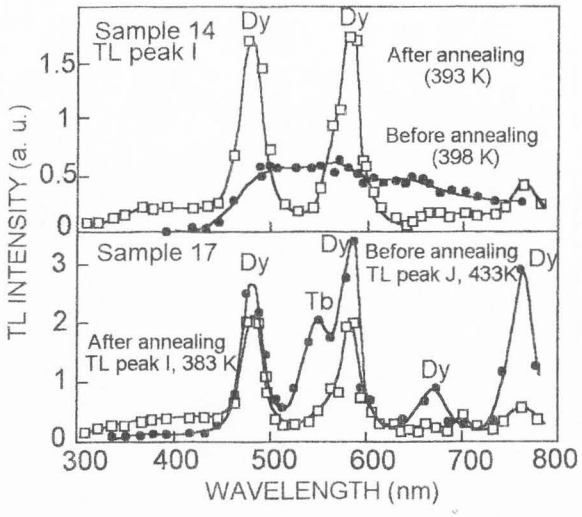

Figure 28. Emission spectra of TL peak I obtained after X-irradiation at RT from two semi-metamict zircons (samples 14 and 17) before and after annealing at 1275K, 24 hours, in air. In sample 17, the peak I does not exist before annealing but appears after annealing and replaces the peak J which disappears.

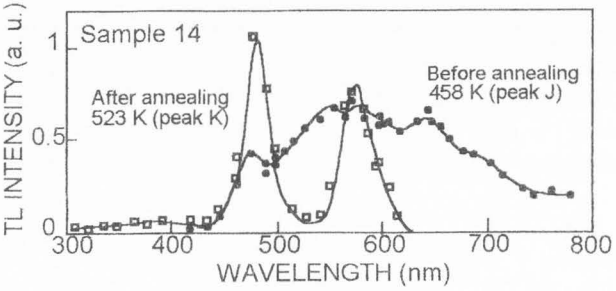

Figure 29. Emission spectra of TL peaks J and K obtained after X-irradiation at RT from the semi-metamict sample 14 before (peak J) and after (peak K) annealing at 1275K, 24 hours, in air. The peak J disappears after annealing and is replaced by peak I.

---

values, the TL age can be calculated. The period covered by the TL dating method stretches from 100 years as far as the last heating of the ceramics [95].

Sutton and Zimmerman [80] have described a radioactive-inclusion technique. It consists to measure the TL presented by highly radioactive grains of zircon which are a minor constituent of most archaeological ceramics. Because of their high radio-active content, the natural radiation dose will be greatly dominated by the internal α-particle dose. The natural dose is determined from TL measurements; the internal dose-rate calculated from the measured U and Th contents and the age thus calculated.

Wintle [100] shows that there is a loss of charge carriers from traps which contribute to the TL of natural zircons in the 625K-725K region. This loss is termed "anomalous fading" [100] and is confirmed by various workers [5, 21, 82, 84]. Templer [82] observes that it occurs equally at all wavelengths between 300-650 nm. Durrani and Amin [21] find that all zircons (natural or synthetic) exhibit anomalous fading. Such fading is aggravated by radiation damage but is reduced on annealing the damaged crystal. A model for the anomalous fading is proposed by Templer [84]. The results indicate that above RT localised transitions occur and at lower temperatures tunnelling predominates.

The anomalous fading effect which leads to an erroneous evaluation of the archaeological age using conventional TL method can be reduced by the phototransfer TL dating technique proposed by Bailiff [5]. This technique consists to transfer the charge carriers captured in the deep traps to the shallow ones by illumination with an appropriate UV light. In zircons, the deep traps are situated at temperature higher than 725K and the phototransfer is made at RT or LNT [6].

The auto-regenerative TL dating method, first proposed by Sutton and Zimmerman [81] and extended then by Templer [83], consists to measure the TL regenerated at RT [81] or at LNT [83, 85], in a certain time (several months), by the high internal radioactivity content of natural zircon grains and to compare it with the natural TL first recorded.

Conclusion

The TL peaks observed in natural and synthetic zircons between 77K and 350K agree fairly well and are explained by the same model involving an energy transfer mechanism from an host lattice emission related to the SiO_4^{4-} groups to doping RE^{3+} elements. Usually, the latter consist of Dy^{3+}. An emission attributed to the presence of OH^- ions is also observed.

At temperatures higher than 350K, natural zircons exhibit various TL peaks generally unobserved in synthetic samples. The presence of different RE^{3+} emissions is interpreted by a charge transfer mechanism involving the trapping of electrons or holes by RE^{3+} with variation of valence states. The existence of a broad band around 600 nm is related to the defects induced by the metamictisation process. Following the recent model of metamictisation, the immediate environment of the Zr^{4+} ion must be highly disturbed, with sufficient variation in Zr-O distances and Zr-O-Si bond angles to destroy the acoustic modes present in crystalline zircon [101]. In contrast, the immediate environment of the Si^{4+} ions must be essentially retained. The variation of interionic distances, refractive indices, optical transmission and dielectric constants affect the TL phenomenon and lead first to a displacement of some TL peaks and an attenuation of their intensities. For the high α-doses, the intensity of TL peaks is dramatically decreased.

References

[1] Ainess RD, Rossman GR (1986) Relation between radiation damage and trace water in zircon, quartz, and topaz. Amer Mineral **71**, 1186-1193.

[2] Aitken MJ, Zimmerman DW, Fleming SJ (1968) Thermoluminescent dating of ancient pottery. Nature (London) **219**, 442-445.

[3] Aitken MJ (1985) Thermoluminescence Dating. Academic Press, London. pp. 172-178.

[4] Akhamanova M, Leonova LL (1961) Investigation of metamictization of zircons with the aid of IR absorption spectra. Geokhimiya **5**, 401-414; translated in Geochemistry (1961), **5**, 416-431.

[5] Bailiff IK (1976) Use of phototransfer for the anomalous fading of thermoluminescence. Nature **264**, 531-533.

[6] Bailiff IK, Bowman SG, Mobbs SF, Aitken MJ (1977) The phototransfer technique and its use in TL dating. J Electrostatics **3**, 269-280.

[7] Bershov LV (1971) Isomorphism of Tb^{4+}, Tu^{2+} and Y^{3+} in zircon. Geokh **1**, 48-53; translated in Geochemistry (1971) **1**, 24-28.

[8] Blasse G (1966) On the Eu^{3+} fluorescence of mixed metal oxides. IV. The photoluminescence efficiency of Eu^{3+} activated oxides. J Chem Phys **45**, 2356-2359.

[9] Blasse G (1970) Some considerations on rare earth activated phosphors. J Lumin **1**, 766-777.

[10] Bragg WL, West J (1926) The structure of beryl. Proc Roy Soc **A111**, 691-714.

[11] Bursill LA, McLaren AC (1966) Transmission electron microscope study of natural radiation damage in zircon. Phys Stat Sol **13**, 331-343.

[12] Cartz L, Fournelle R (1979) Metamict zircon formed by heavy ion bombardment. Rad Effects **41**, 211-217.

[13] Caruba R, Turco G, Iacconi P, Keller P (1974) Solution solide d'éléments de transition trivalents dans le zircon et l'oxyde de zirconium. Etude par thermoluminescence artificielle. (Solid solution of trivalent transition elements in zircon and zirconium oxide. Study by thermoluminescence). Bull Soc fr Minéral Cristallogr **97**, 278-283.

[14] Caruba R, Iacconi P (1983) Les zircons des pegmatites de Narssârssuk (Groënland). L'eau et les groupements OH dans les zircons métamictes. {The pegmatic zircons of Narssârssuk (Groënland). Water and hydroxyl groups in metamict zircons}. Chem Geol **38**,

75-92.

[15] Caruba R, Baumer A, Ganteaume M, Iacconi P (1985) An experimental study of hydroxyl groups and water in synthetic and natural zircons: A model of the metamict state. Amer Mineral **70**, 1224-1231.

[16] Chee J, Oczowski HL, Kirsh Y, Scott A, Siyanbola WO, Townsend PD (1988) TL spectra of natural zircons. Nucl Tracks Radiat Meas **14**, 35-42.

[17] Chakoumakos BC, Murakami T, Lumpkin GR, Ewing RC (1987) Alpha-decay-induced fracturing in zircon: The transition from the crystalline to the metamict state. Science **236**, 1556-1559.

[18] Curie D (1957) Modèles pour les divers types de pièges dans le ZnS phosphorescent. Libération thermique et optique des électrons piégés. (Models for the various kinds of traps in ZnS. Thermal and optical release of the trapped electrons). J Phys Rad **18**, 214-222.

[19] Dawson P, Hargreave MM, Wilkinson GR (1971) The vibrational spectrum of zircon. J Phys C: Solid St Phys **4**, 240-256.

[20] Dieke GH (1968) Spectra and Energy Levels of Rare Earth Ions in Crystals. Interscience, New York. pp. 1-115.

[21] Durrani SA, Amin YM (1985) Radiation damage and the anomalous fading of TL in natural and artificial zircons. Nucl Tracks **10**, 539-546.

[22] Duschesne JC, Caruba R, Iacconi P (1987) Zircon in charnockitic rocks from Rogaland (southwest Norway): Petrogenetic implications. Lithos **20**, 357-368.

[23] Ewing RC, Chakoumakos BC, Lumpkin GR, Murakami T (1987) The metamict state. Mat Res Soc Bul **15**, 58-66.

[24] Farges F, Calas G (1991) Structural analysis of radiation damage in zircon and thorite: An X-ray absorption spectroscopic study. Amer Mineral **76**, 60-73.

[25] Fedorovskikh Yu, Gavrilov FF, Shorikov OG, Shulg'in BV, Polezaev Yu (1972) Radioluminescence of zircon. Izv Vyss Ucheb Zav, Fizika **10**, 148-149; translated in Sov Phys J (1972) **10**, 1521-1522.

[26] Fedorovskikh Yu, Shulg'in BV, Gavrilov FF, Polezaev Yu, Antonov AV (1972) Cathodic luminescence of zirconium containing phosphors. Zh Prikl Spekst **17**, 364-367; translated in J Appl Spect (1972) **17**, 1104-1106.

[27] Fedorovskikh Yu, Shulg'in BV, Emel'chenko GA, Gavrilov FF, Ilyukhin VV (1973) Crystal structure and optical spectra of zircon. Izv Akad Nauk SSSR, Neorg Mat **9**, 432-434; translated in Inorg Mat (1972) **9**, 384-386.

[28] Fielding PE (1969) Site symmetry of RE^{3+} in flux-grown zircon. Australia J Chem **22**, 2463-2465.

[29] Fielding PE (1970) Colour centres in zircon containing both Eu^{3+} and U^{4+} ions. Aust J Chem **23**, 1513-1521.

[30] Frondel C, Collette RL (1957) Hydrothermal synthesis of zircon, thorite and huttonite. Amer Mineral **42**, 759-765.

[31] Gaft M, Zhukova VA, Rassulov VA, Rakov LT (1986) Nature of photoluminescence in zircon (in Russian). Mineral Zh **8**, 74-78.

[32] Godfrey-Smith DI, McMullan WG, Huntley DJ, Thewalt ML (1989) Time-dependent recombination luminescence spectra arising from optical ejection of trapped charges in zircons. J Lumin **44**, 47-57.

[33] Headley TJ, Ewing RC, Haaker RF (1981) High resolution study of the metamict state in zircon. Proc. of 1981 Annual Meet. Electron Micros. Soc Am San Francisco Press, CA. pp. 112-113.

[34] Headley TJ, Arnold GW, Northrup CJM (1982) Dose dependence of Pb-ion implantation damage in zirconolite, hollandite, and zircon. In: Scientific Basis for Radioactive Waste Management. Vol. 11. Lutze W (ed.). North-Holland, New York. pp. 379-388.

[35] Holland HD, Gottfried D (1955) The effect of nuclear radiation on the structure of zircon. Acta Cryst **8**, 291-300.

[36] Hurley PM, Fairbairn HW (1953) Radiation damage in zircon: A possible age method. Bull Geol Soc Am **64**, 659-674.

[37] Hutton DR, Milne RJ (1969) Paramagnetic resonance of Tb^{4+} in zircon. J Phys C: Solid St Phys **2**, 2297-2300.

[38] Iacconi P, Caruba R, Keller P and Turco G (1975) Thermoluminescence de zircons et de malacons naturels. Influence de la température et de la pression. (Thermoluminescence of natural zircons and malacons. Role of temperature and pressure). Mod Geol **5**, 177-184.

[39] Iacconi P, Caruba R (1977) Sur le rôle des OH^- dans l'émission de thermoluminescence du zircon $Zr(SiO_4)_{1-x}OH_{4x}$ synthétique. (Role of OH^- groups in the thermoluminescent emission of synthetic zircon $Zr(SiO_4)_{1-x}OH_{4x}$). C.R. Acad Sc Paris **285**, 227-229.

[40] Iacconi P (1979) Etude et interprétation des propriétés thermoluminescentes des zircons $ZrSiO_4$ et $Zr(SiO_4)_{1-x}OH_{4x}$ dopés par des éléments trivalents de la série des lanthanides. Rôle du groupement hydroxyl et des inclusions de ZrO_2. (Thermoluminescent properties of zircons $ZrSiO_4$ and $Zr(SiO_4)_{1-x}OH_{4x}$ doped with individual trivalent rare earth elements of the lanthanide series. Influence of hydroxyl groups and ZrO_2 inclusions). Thèse d'Etat. Université de Nice.

[41] Iacconi P, Deville A, Gaillard B (1980) Trapping and emission centres in X-irradiated zircon. I. Contribution of the OH^- ion. Phys Stat Sol (a) **59**, 139-146.

[42] Iacconi P, Deville A, Gaillard B (1980) Trapping and emission centres in X-irradiated zircon. II. Contribution of the SiO_4^{4-} groups. Phys Stat Sol (a) **59**,

639-646.

[43] Iacconi P, Caruba R (1980) Trapping and emission centres in X-irradiated zircon. III. Influence of trivalent rare-earth impurities. Phys Stat Sol (a) **62**, 589-596.

[44] Iacconi P, Caruba R (1984) Trapping and emission centres in X-irradiated natural zircon. Characterisation by thermoluminescence. Phys Chem Minerals **11**, 195-203.

[45] Iacconi P, Lapraz D, Barthe J, Keller P, Portal G (1984) Thermoluminescence dosimetric properties of natural zircon ($ZrSiO_4$). Radiat Prot Dosim **6**, 189-192.

[46] Iacconi P, Lapraz D, Orlans P, Daviller D, Guilhot B (1990) Characterisation of ceramics by thermoluminescence and exoelectronic emission. Ceram Intern **16**, 327-245.

[47] Jain VK (1977) Some aspects of the thermoluminescence of zircon (sand) and zirconia. Indian J Pure Appl Phys **15**, 601-605.

[48] Jain VK (1978) Thermoluminescence glow curve and spectrum of zircon (sand). Bull Mineral **101**, 358-362.

[49] Kirsh Y, Townsend PD (1987) Electron and hole centres produces in zircon by X-irradiation at room temperature. J Phys C: Solid St Phys **20**, 967-980.

[50] Krasnobaev AA (1964) On thermoluminescence in zircon (in Russian). Kapiski Vses Mineral Obshch **93**, 713-720.

[51] Kulp JL, Volchok HL, Holland HL (1952) Age from metamict minerals. Amer Mineral **37**, 709-718.

[52] Lehmann W (1972) Activators and co-activators in calcium sulfide phosphors. J Lumin **5**, 87-107.

[53] Lehmann W (1973) Calcium oxide phosphors. J Lumin **6**, 455-470.

[54] Leverenz HW (1950) Luminescence of solids. John Wiley, New York. pp. 127-245.

[55] Marfunin AS (1979) Physics of Minerals and Inorganic Materials. Springer-Verlag, New York. p. 280.

[56] McDougall DJ (ed.) (1968) Thermoluminescence of Geological Materials. Academic Press, London. pp. 530-531.

[57] McKeever SWS (1985) Thermoluminescence of Solids. Cambridge Univ. Press, London. pp. 1-371.

[58] Murakami T, Chakoumakos BC, Ewing RC (1986) X-ray powder diffraction analysis of alpha-event radiation damage in zircon. In: Advances in Ceramics. Vol. 20: Nuclear Waste Management II. Clark DE, White WB, Machiels J (eds.). American Cancer Society, Columbus, Ohio. pp. 745-753.

[59] Murakami T, Chakoumakos BC, Ewing RC, Lumpkin GR, Weber WJ (1991) Alpha-decay event damage in zircon. Amer Mineral **76**, 9-10, 1510-1532.

[60] Mursic Z, Vogt T, Boysen H, Frey F (1992) Single-crystal neutron diffraction of metamict zircon up to 2000K. J Appl Cryst **25**, 519-523.

[61] Mursic Z, Vogt T, Frey F (1992) High temperature neutron powder diffraction study of zircon up to 1900K. Acta Cryst **B48**, 584-590.

[62] Nerurkar AP, De R, Chakraborty PN, Kaul IK (1979) Studies on thermoluminescence, metamictization and sintering properties of zircon sands. Modern Geol **7**, 13-24.

[63] Nicholas JV (1967) Origin of the luminescence in natural zircon. Nature **215**, 1476.

[64] Oberhofer M, Scharmann A (1981) (eds.) Applied Thermoluminescence Dosimetry. Adam Hilger Ltd., Bristol, U.K. pp. 1-390.

[65] Ovcharenko VK, Eryomenko GK (1970) Luminescence of zircon from the rocks of the October alkaline massif (in Russian). Koustit Svojsta Miner **4**, 58-62.

[66] Pabst A (1952) The metamict state. Amer Mineral **37**, 137-157.

[67] Pauling L (1960) The Nature of Chemical Bond. Cornell Univ. Press, New York. pp. 1-50.

[68] Pellas P (1965) Etude sur la recristallisation thermique des zircons naturels. (The study of thermal recrystallization of natural zircon). Mem Mus Nat Hist Nat Paris **12**, 227-253.

[69] Reisfeld R (1972) Inorganic ions in glasses and polycrystalline pellets as fluorescence standard reference materials. J Res NBS A: Phys Chem **76A**, 613-635.

[70] Remond G, Cesbron F, Chapoulie R, Ohnenstetter D, Roques-Carmes C, Shvoerer M (1992) Cathodoluminescence applied to the microcharacterisation of mineral materials: A present status in experimentation and interpretation. Scanning Microsc **6**, 23-68.

[71] Reynolds RW, Boatner IA, Finch CB, Chatelain A, Abraham MM (1972) EPR investigations of Er^{3+}, Yb^{3+}, and Gd^{3+} in zircon structure silicates. J Chem Phys **56**, 5607-5625.

[72] Robinson K, Gibbs GV, Ribbe PH (1971) The structure of zircon: A comparison with garnet. Amer Mineral **56**, 782-790.

[73] Samoilovitch MI, Novozhilov AI, Barsanov GP (1968) EPR on irradiated crystals of zircon with various impurities. Geokh **4**, 494-495; translated in Geoch Int (1968) **5**, 420-422.

[74] Shinno I (1987) Color and photoluminescence of rare earth element-doped zircon. Mineral J **13**, 239-253.

[75] Shulg'in BV, Fedorovskikh Yu, Krasnobaev AA, Polezaev Yu (1974) The thermostimulated luminescence of natural zircon. Zh Prikl Spektrosk **21**, 470-474; translated in J Appl Spect **21**, 435-439.

[76] Solntsev VP, Shcherbakova MY (1972) Electron spin resonances of Ti^{3+} in α-quartz and zircon. Zh

Strukt Khim **13**, 924-927; translated in J Struct Chem (1972), **13**, 859-861.

[77] Solntsev VP, Shcherbakova MY (1973) ESR study on the structural defects in irradiated zircons. Dokl Akad Nauk SSSR **212**, 156-158; translated in Dokl Phys Chem (1973) **212**, 731-733.

[78] Solntsev VP, Shcherbakova MY, Dvornikov (1974) SiO_2^-, SiO_3^{3-}, SiO_4^{5-} radicals in the $ZrSiO_4$ structure, from EPR data. Zh Strukt Khim **15**, 217-221; translated in J Struct Chem (1974) **15**, 201-204.

[79] Speer JA (1980) Zircon. In: Orthosilicates. 2nd ed. Reviews in Mineralogy, Vol. **5**. Ribbe PH (ed.). Mineralogical Society of America, Washington, DC. pp. 67-112.

[80] Sutton SR, Zimmerman DW (1976) Thermoluminescent dating using grains from archaeological ceramics. Archaeometry **18**, 125-134.

[81] Sutton SR, Zimmerman DW (1979) The zircon natural method: Initial results and low level thermoluminescence measurements. PACT **3**, 465.

[82] Templer RH (1985) The dating of zircons by autoregenerated TL at low temperatures. Nucl Tracks **10**, 789-798.

[83] Templer RH (1985) The removal of anomalous fading in zircon. Nucl Tracks **10**, 531-537.

[84] Templer RH (1986) The localised transition model of anomalous fading. Rad Prot Dosim **17**, 1-4, 493-497.

[85] Templer RH, Smith BW (1988) Auto-regenerative TL dating with zircon inclusions from fired materials. Nucl Tracks Radiat Meas **14**, 329-332.

[86] Vance ER, Anderson BW (1972) Study of metamict Ceylon zircons. Mineral Mag **38**, 605-613.

[87] Vance ER (1975) α-recoil damage in zircon. Rad Effects **24**, 1-6.

[88] Vance ER, Boland JN (1975) Fission fragment damage in zircon. Rad Effects **26**, 135-139.

[89] Vance ER, Efstathiou L, Hsu FH (1980) X-ray and positron annihilation studies of radiation damage in natural zircons. Rad Effects **52**, 61-68.

[90] Vaz E, Sentfle F (1971) Geologic and dating of zircon using thermoluminescence. Mod Geol **2**, 239-245.

[91] Vaz JE, Senftle FE (1971) Thermoluminescence study of the natural radiation damage in zircon. J Geophys Res **76**, 2038-2050.

[92] Vinokurov VM, Gainullina NM, Evgrafova LA, Nizamutdinov NM, Suslina AN (1971) $Zr^{4+} \rightarrow Y^{3+}$ isomorphism in zircon and the associated charge compensation. Sov Phys Cryst **16**, 262-265; translated from Kristall. (1971) **16**, 318-323.

[93] Votyakov SL, Krokhalev VY, Krasnobaev AA (1985) Zircon recombination luminescence. Zh Prikl Spektr **42**, 928-935; translated in J Appl Spectr (1985) **42**, 633-638.

[94] Votyakov SL, Ivanov IP, Krasnobaev AA, Krokhalev VY, Korzhinskaya VS (1986) Luminescence spectral properties of zirconium orthosilicate prepared by hydrothermal method. Izv Akad Nauk SSSR, Neorg Mat **22**, 281-286; translated in Inorg Mat (1986) **22**, 239-244.

[95] Wagner GA (1979) Archaeometric dating. In: Lectures in Isotope Geology. Jäger E, Hunziker JC (eds.). Springer-Verlag, Berlin. pp. 178-188.

[96] Wang LM, Ewing RC, Weber WJ, Eby RK (1993) Temperature and ion-mass dependence of amorphization dose for ion beam irradiated zircon ($ZrSiO_4$). Mat Res Symp Proc **279**, 451-456.

[97] Wasilewski PJ, Senftle FE, Vaz JE, Thorpe AN, Alexander CC (1973) A study of the natural α-recoil damage in zircon by IR spectra. Rad Effects **17**, 191-199.

[98] Weber WJ (1991) Self-radiation damage and recovery in Pu-doped zircon. Rad Effects and Defects in Solids **115**, 341-349.

[99] Weber WJ, Ewing RC, Wang LM (1994) The radiation-induced crystalline-to-amorphous transition in zircon. J Mater Res **9**, 688-698.

[100] Wintle AG (1973) Anomalous fading of thermoluminescence in mineral samples. Nature **245**, 143-144.

[101] Woodhead JA, Rossman GR, Silver LT (1991) The metamictization of zircon: Radiation dose-dependent structural characteristics. Amer Mineral **76**, 74-82.

[102] Wyckoff RWG (1965) Crystal Structures. Vol. 3. John Wiley, New York. p. 15.

[103] Yada KY, Tanji T, Sunagawa I (1981) Application of lattice imagery to radiation damage investigation in natural zircon. Phys Chem Minerals **7**, 47-52.

[104] Yada K, Tanji T, Sunagawa I (1987) Radiation induced lattice defects in natural zircon observed at atomic resolution. Phys Chem Minerals **14**, 197-204.

[105] Yang B, Luff BJ, Townsend PD (1992) Cathodoluminescence of natural zircons. J Phys: Condens Matter **4**, 5617-5624.